Global Change Biology

Global Change Biology (2012) **18**, 2925–2944, doi: 10.1111/j.1365-2486.2012.02757.x

Assessing the effects of nitrogen deposition and climate on carbon isotope discrimination and intrinsic water-use efficiency of angiosperm and conifer trees under rising CO_2 conditions

STEFANO LEONARDI*, TIZIANA GENTILESCA†, ROSSELLA GUERRIERI‡, FRANCESCO RIPULLONE†, FEDERICO MAGNANI§, MAURIZIO MENCUCCINI‡, TWAN V. NOIJE¶ and MARCO BORGHETTI†‖

*Dipartimento di Scienze Ambientali, Università di Parma, via G. P. Usberti 11, 43100, Parma, Italy, †Department of Crop Systems, Forest and Environmental Sciences, University of Basilicata, viale dell'Ateneo Lucano 10, 85100, Potenza, Italy, ‡School of GeoSciences, University of Edinburgh, Crew Building, West Mains Road, EH9 3JN, Edinburgh, United Kingdom, §Department of Fruit and Trees, University of Bologna, via Fanin 43, 40100, Bologna, Italy, ¶Royal Netherlands Meteorological Institute (KNMI), PO Box 201, 3730 AE, De Bilt, The Netherlands, ‖Department of Crop Systems, Forest and Environmental Sciences, University of Basilicata, viale dell'Ateneo Lucano 10, 85100, Potenza, Italy

Abstract

The objective of this study is to globally assess the effects of atmospheric nitrogen deposition and climate, associated with rising levels of atmospheric CO_2, on the variability of carbon isotope discrimination ($\Delta^{13}C$), and intrinsic water-use efficiency (*iWUE*) of angiosperm and conifer tree species. Eighty-nine long-term isotope tree-ring chronologies, representing 23 conifer and 13 angiosperm species for 53 sites worldwide, were extracted from the literature, and used to obtain long-term time series of $\Delta^{13}C$ and *iWUE*. $\Delta^{13}C$ and *iWUE* were related to the increasing concentration of atmospheric CO_2 over the industrial period (1850–2000) and to the variation of simulated atmospheric nitrogen deposition and climatic variables over the period 1950–2000. We applied generalized additive models and linear mixed-effects models to predict the effects of climatic variables and nitrogen deposition on $\Delta^{13}C$ and *iWUE*. Results showed a declining $\Delta^{13}C$ trend in the angiosperm and conifer species over the industrial period and a 16.1% increase of *iWUE* between 1850 and 2000, with no evidence that the increased rate was reduced at higher ambient CO_2 values. The temporal variation in $\Delta^{13}C$ supported the hypothesis of an active plant mechanism that maintains a constant ratio between intercellular and ambient CO_2 concentrations. We defined linear mixed-effects models that were effective to describe the variation of $\Delta^{13}C$ and *iWUE* as a function of a set of environmental predictors, alternatively including annual rate (N_{rate}) and long-term cumulative (N_{cum}) nitrogen deposition. No single climatic or atmospheric variable had a clearly predominant effect, however, $\Delta^{13}C$ and *iWUE* showed complex dependent interactions between different covariates. A significant association of N_{rate} with *iWUE* and $\Delta^{13}C$ was observed in conifers and in the angiosperms, and N_{cum} was the only independent term with a significant positive association with *iWUE*, although a multi-factorial control was evident in conifers.

Keywords: Nitrogen deposition, Carbon isotope discrimination, Water-use efficiency, Carbon dioxide, Tree ring, Climate, Forest, Linear Mixed-Effect Model

Received 19 November 2011; revised version received 28 May 2012 and accepted 29 May 2012

Introduction

Global change can profoundly alter forest ecosystem carbon balance by the direct effect of increasing atmospheric CO_2 on photosynthesis as well as through indirect effects, particularly increased temperatures and altered precipitation patterns caused by accumulating green-house gas levels (Schimel *et al.*, 2001). The potential for forests to functionally adjust to these changes may substantially affect the capacity of terrestrial ecosystems to take up carbon under future climatic conditions. This functional response, that can represent an important climate forcing, remains highly uncertain (Bonan, 2008; Serengil *et al.*, 2011).

Among other functional traits involved in the response of forest to global change, plant water-use efficiency, bridging carbon and water cycling, is

Correspondence: Marco Borghetti, tel. + 39 0971 205 246, fax + 39 0971 205 378, e-mail: marco.borghetti@unibas.it

reported to have an important role (Jackson *et al*., 2005). However, knowledge of how water-use efficiency is impacted by climatic and atmospheric changes at different scales remains incomplete. To date, the global change attributes that have received the most attention with respect to potential influences on plant water-use efficiency include alterations in precipitation patterns, temperature, and atmospheric CO_2 increase (e.g. Oliver *et al*., 2009; Guo *et al*., 2010).

One of the most considerable atmospheric changes at the global scale is the anthropogenic perturbation of the nitrogen (N) cycle, due to fossil-fuel combustion and agricultural emissions (Galloway *et al*., 2008; Gruber & Galloway, 2008). Approximately 18×10^6 kg of reactive N is globally deposited into forests each year, with marked regional differences in annual deposition rate (Schlesinger, 2009). In recent years, a beneficial role of N deposition on forest productivity, and on the terrestrial C sink has been suggested (Norby, 1998; Magnani *et al*., 2007; Thomas *et al*., 2010), although the magnitude of this effect is the subject of an intensive debate (Sutton *et al*., 2008; Pregitzer *et al*., 2008).

We hypothesize that N deposition can have an effect on the balance between water loss and carbon gain at the leaf level, the so-called intrinsic water-use efficiency (*iWUE*). This may be the consequence of changes in leaf N concentration, which can in turn affect the ratio between assimilation and stomatal conductance. The relationship between leaf N concentration and *iWUE* is not straightforward, but a positive trend is often observed, in ambient air (*e.g.* Guehl *et al*., 1995; Ripullone *et al*., 2004) as well as in elevated CO_2 (Tognetti & Johnson, 1999). A review on the effects of nutrient supply in crop plants emphasized the importance of N influence on *iWUE* (Brueck, 2008).

Nitrogen deposition can enhance leaf nutritional status by different ecological mechanisms. For example, most N deposition over forests is initially intercepted and taken up by tree canopies. The N retention by canopies varies largely and is reported up to 70% of N deposition (Gaige *et al*., 2007; Dail *et al*., 2009; Sievering *et al*., 2007). Nitrogen made available to trees through canopy uptake can subsequently be directly used in plant metabolism (Sparks, 2009). In a recent experiment canopy nitrogen application was associated with increased tree *iWUE* (Guerrieri *et al*., 2011). Atmospheric N deposition can also determine long-term effects on soil fertility mediated by the accumulation of N in the soil, causing a change in soil organic matter stoichiometry (lower C/N ratio). The decline in the C/N ratio can stimulate N mineralization and N plant uptake, and N leaching if a specific saturation threshold is overcome (Aber *et al*., 2003).

Tree ring studies, using $^{13}C/^{12}C$ ratio in dated growth rings, provide long-term carbon isotope chronologies to explore the relationship between environmental variability and changes in tree physiology, with special reference to the balance between water loss and carbon gain at the leaf level (Loader *et al*., 2007; Saurer & Siegwolf, 2007; for reviews). However, even in recent efforts to describe leaf $^{13}C/^{12}C$ variability in woody plants at the global scale (Diefendorf *et al*., 2010; Kohn, 2010), the potential atmospheric N deposition effects have been neglected.

Studies to define predictive relationships between environmental variables and plant carbon discrimination (or *iWUE*) using tree ring isotope chronologies must also consider the potential effect of rising CO_2 atmospheric concentration over the industrial period, from 280 to 380 μmol mol^{-1} during the last 150 years (IPPC, 2007). Higher ambient CO_2 concentrations might enhance photosynthesis and constrain transpiration, as stomata tend to close under elevated CO_2 (Ainsworth & Rogers, 2007), leading to increased *iWUE*, as evidenced by long-term tree ring isotope chronologies (Peñuelas *et al*., 2011). Saurer *et al.* (2004) proposed useful hypothetical scenarios to interpret possible responses of plant carbon isotope discrimination to increased CO_2 levels, but a global comparison of observational data with hypothetical patterns, including both angiosperm and conifer tree species, remains unavailable.

The aim of this study was to assess temporal changes in carbon isotope discrimination and *iWUE* in relation to climate and major global changes, particularly increased CO_2 and N deposition. We investigated the following hypothesis: atmospheric N deposition is a significant factor in determining global scale variability in plant carbon isotope discrimination and *iWUE* in angiosperm and conifer trees under rising CO_2 conditions. The variation in carbon discrimination and *iWUE* was calculated from carbon isotope tree-ring chronologies obtained from the literature, and correlated with increased atmospheric CO_2 data for the period 1850–2000 and with atmospheric N deposition and climatic variables for the period 1950–2000, for a large number of sites worldwide.

Materials and methods

Data mining and selection

We obtained more than 30 studies reporting carbon isotope ratio $^{13}C/^{12}C$ ($\delta^{13}C_p$) from long-term time-series dated woody rings of angiosperm and conifer trees growing at different sites throughout the world. $\delta^{13}C_p$ was expressed as the relative deviation from the international standard, Vienna Pee Dee Belemnite (VPDB) (IAEA, 1995):

$$\delta^{13}C_p = \left(\frac{^{13}C/^{12}C_{wood}}{^{13}C/^{12}C_{VPDB}} - 1\right) \cdot 1000 \quad (1)$$

Literature searches were first conducted using the ISI Web of Science database. We conducted an inquiry for primary literature studies, and the cited literature. We particularly looked for studies that addressed tree-ring research conducted at sites located in areas with contrasting rates of annual N deposition, using published maps of gridded simulated data (*e.g.* Dentener *et al.*, 2006). On the basis of site and stand description in the original studies, we selected cases where evidence of manipulation or disturbance (soil fertilization, logging, fires etc.) was not reported. We restricted the study species to canopy trees and excluded data that corresponded to the juvenile growing phase, when this data was explicitly reported in the article. Studies published until April 2010 were considered for selection. If available in tabular form in the original studies, $\delta^{13}C_p$ values were manually digitized; if provided in graphical form, $\delta^{13}C_p$ values were obtained from graph curves using the Un-Scan-It 5.0 software (Silk Scientific, Orem, UT, USA). Interpolation was not applied in any case.

A total of 89 isotope tree-ring chronologies were assembled, representing 36 tree species (23 conifer and 13 angiosperm species) from 53 sites throughout the world; more than 80% of the sites were represented by $\leq$ 2 chronologies. The number of trees combined in single chronologies varied among sites (Table 1). In most cases, the source material for $\delta^{13}C_p$ analysis was cellulose. In some cases, isotope chronologies were not developed on single annual rings, but different wood rings were pooled to obtain sufficient material for the analysis, *e.g.* 5-year wood rings groups. $\delta^{13}C_p$ values were always used, as reported and dated in the original publication.

Latitude of selected sites ranged between 67° N and 41° S and sites spanned different biomes, based on world biomes map (De Blij *et al.*, 2004): taiga (8%), temperate (60%), chaparral (9%), rainforest (8%), and desert (15%) (Table 1). Mean site latitude and tree age for the more intensively analyzed period (1950–2000) are reported in Table S1.

Climatic variables

For each site, annual climatic variable values for 1950–2000 were extracted from the 0.5 × 0.5 degree CRU TS 2.1 global climatic gridded dataset available for download from the Climatic Research Unit of University of East Anglia, Norwich, UK (www.cru.uea.ac.uk/cru/data/hrg/). The selected sites exhibited a large range of climatic conditions, indicated by broad mean annual temperature (T_m) gradients, total annual precipitation (P), and number of wet days (D_w). T_m ranged between −21.9 and 25.7 °C, and P between 26 and 3364 mm (average for 1950–2000). However, these variables did not reveal appreciable long-term temporal patterns for 1950–2000 at the selected sites (Fig. S1).

Annual atmospheric CO_2 concentration (C_a) values, and the atmospheric CO_2 carbon isotope ratio ($\delta^{13}C_a$) from 1850 to 2000 were obtained from McCarroll & Loader (2004). According to these data, C_a showed a respective increase from 285 to 312, and 312 to 368.5 μmol mol^{-1} from 1850 to 1950 and from 1950 to 2000. Concurrent with C_a increase, $\delta^{13}C_a$ decreased from −6.41 to −6.86‰ and −6.86 to −7.99 ‰ during the same years, as a consequence of the admixture of large amounts of fossil-fuel derived CO_2. We assume the canopy of overstory trees experienced well mixed atmospheric conditions, and a single value of C_a can be applied to different sites in a given year.

Atmospheric deposition

The annual total reactive N deposition at the selected sites for the years 1960–2000 was estimated from a TM4 chemistry-transport model simulation, conducted as part of the EU RETRO project (Schultz *et al.*, 2007). Total reactive N includes oxidized reactive components (NO_y, also including peroxyacyl nitrates (PAN) and organic nitrates), and reduced reactive compounds (NH_x, including both ammonia NH_3 and ammonium NH_4). For this simulation, the model was driven by meteorological data from the ERA-40 reanalysis from the European Centre for Medium-Range Weather Forecasts (ECMWF) at a horizontal resolution of 3 × 2 degrees (longitude x latitude). The TM4 results have been extrapolated back in time for 1950–1959 using decadal emissions estimates from the EDGAR-HYDE dataset (van Aardenne *et al.*, 2001). The deposition rates for this time period were estimated at the 1960–1969 simulated deposition, scaled by the annual nitrogen emissions relative to the 1960s, where we assumed emissions changed linearly from 1950 to 1959. The scaling factors were derived at the TM4 3 × 2 degree, and the original 1 × 1 degree emission data of the EDGAR-HYDE inventory were initially coarsened to this resolution. Deposition rates were set to zero in model grid cells with zero nitrogen emissions from 1960–1969. Finally, we interpolated the results to a 0.5 × 0.5 degree grid, and each site was associated with the N deposition value of the corresponding grid cell.

From the same model simulation, the sulfur (SO_x = SO_2+SO_4) and ozone (O_3) deposition fields were also extracted for 1950–2000 (SO_x), and 1960–2000 (O_3), using the same interpolation method.

Relationship between carbon isotope discrimination and intrinsic water-use efficiency

The potential of carbon isotope chronologies to act as effective physiological archives is a consequence of two independent processes: *i*) the heavier carbon isotope (^{13}C) depletion in plant material relative to atmospheric CO_2, which is due to isotope fractionations that occur during CO_2 diffusion into the leaf, and during carboxylation by Rubisco; *ii*) the relationship between carbon isotope discrimination ($\Delta^{13}C$) and the ratio between the concentration of CO_2 in leaf intercellular spaces and in the atmosphere, which is related to changes in assimilation or stomatal conductance (Farquhar *et al.*, 1989). Post photosynthetic fractionations (Cernusak *et al.*, 2009) can partially reduce the degree to which the primary isotope signal imprinted in leaf organic matter is recorded in woody tissues, however, carbon isotope ratio in tree rings still contains useful information on plant gas exchanges, once long-term changes

Table 1 Data set characteristics: tree species, geographic coordinates (*Lat*: latitude; *Long*: longitude); tree ring chronology time intervals (*Int*); source material (*Sou*; C: cellulose; B: bulk wood) for $\delta^{13}C$ analysis; *N* = number of trees combined to obtain tree ring chronologies; biome (*Bio*; Cha: Chaparral; Des: Desert; Rai: Rain forest; Tai: taiga; Tem: temperate forest; Tun: tundra) and literature references (*Ref*). Superscript to latin binomial: 1 = conifer species; 2 = angiosperm species

Tree species	Lat	Lon	Int	Sou	N	Bio	Ref
Abies alba[1]	46°45′N	5°40′E	1860–1980	C	10	Tem	Bert *et al.* (1997)
Acer pseudoplatanus[2]	40°49′N	14°26′E	1851–2004	C	10	Tem	Battipaglia *et al.*, 2007;
Cedrela odorata[2]	10°09′ S	59°26′ W	1855–1995	C	37	Rai	Hietz *et al.* (2005)
Cryptomeria japonica[1]	30°24′ N	130°30′ E	1757–1997	C	1	Rai	Kitagawa & Matsumtoto (1993)
Cryptomeria japonica[1]	30°17′ N	130°35′ E	1833–1988	C	1	Rai	Kitagawa & Matsumtoto (1993)
Crypt. japonica[1], *Abies firma*[1]	35°22′ N	138°56′ E	1947–1995	C	2	Tem	Sakata & Kiyoshi (2000)
Pseudotsuga menziesii[1]	48°21′ N	116°50′ W	1905–1989	C	8	Tem	Monserud & Marshall (2001)
Fagus crenata[2]	35°26′ N	139°02′ E	1945–1996	C	7	Tem	Sakata *et al.* (2001)
Fagus sylvatica[2]	41°56′ N	2°32′ E	1918–2002	B	5	Tem	Peñuelas *et al.* (2008)
Fagus sylvatica[2]	47°N	7°29′ E	1935–1989	C	15	Tem	Saurer *et al.* (1997)
Fagus sylvatica[2]	40°49′N	14°26′E	1916–2004	C	12	Tem	Battipaglia *et al.* (2007)
Fitzroya cupressoides[1]	39°49′ S	73°15′ W	1753–1978	C	1	Tem	Stuiver *et al.* (1984)
Fitzroya cupressoides[1]	41°30′ S	72°33′ W	1700–1987	C	5	Tem	Leavitt & Lara (1994)
Juniperus phoenicea[1]	30°40′ N	34°00′ E	1804–1968	C	1	Des	Epstein & Krishnamurthy (1990)
Juniperus phoenicea[1]	30°40′ N	34°00′ E	1547–1965	C	1	Des	Feng & Epstein (1995)
Larix cajanderi[1]	63°06′ N	139°05′ E	1613–2000	C	10	Tai	Kirdyanov *et al.* (2008)
Larix sibirica[1]	52°18′ N	104°21′ E	1939–1998	C	5	Tai	Voronin *et al.* (2001)
Picea abies[1]	47°10′ N	8°15′ E	1914–1994	C	4	Tem	Anderson *et al.* (1998)
Picea abies[1]	46°25′N	7°49′ E	1956–1995	C	4	Tem	Treydte *et al.* (2001)
Picea sitchensis[1]	57°55′ N	152°36′ W	1885–1979	C	1	Tai	Stuiver *et al.* (1984)
Pinus coulteri[1]	34°12′ N	117°45′ W	1946–1990	C	1	Cha	Feng & Epstein (1995)
Pinus densiflora[1]	37°50′ N	128°25′ E	1937–2000	B	3	Tem	Choi *et al.* (2005)
Pinus edulis[1]	37°26′ N	112°28′ W	1751–1985	C	4	Des	Leavitt & Long (1988)
Pinus edulis[1]	37°30′ N	108°20′ W	1750–1985	C	4	Des	Leavitt & Long (1988)
Pinus edulis[1]	39°52′ N	110°13′ W	1580–1985	C	15	Des	Leavitt & Long (1989)
Pinus edulis[1]	40°41′ N	115°27′ W	1620–1985	C	8	Des	Leavitt & Long (1989)
Pinus longaeva[1]	37°26′ N	118°10′ W	1805–1980	C	4	Des	Leavitt & Long (1992)
Pinus longaeva[1]	37°26′ N	118°10′ W	1529–1965	C	1	Des	Feng & Epstein (1995)
Pinus monticola[1]	48°21′ N	116°50′ W	1912–1989	C	10	Tem	Monserud & Marshall (2001)
Pinus ponderosa[1]	35°55′ N	121°22′ W	1822–1883	C	1	Cha	Leavitt & Long (1988)
Pinus ponderosa[1]	48°21′ N	116°50′ W	1910–1989	C	10	Tem	Monserud & Marshall (2001)
Pinus sylvestris[1]	67°45′ N	33°45′ E	1934–1998	C	3	Tai	Kremenetski *et al.* (2004)
Platanus hybrida[2]	38°06′ N	13°21′ E	1881–1996	B	3	Cha	Dongarrà & Varrica (2002)
Quercus alba[2]	44°33′ N	79°60′ W	1890–2000	C	2	Tem	Bukata & Kyser (2007)
Quercus alba[2]	44°26′ N	76°40′ W	1878–2002	C	3	Tem	Bukata & Kyser (2007)
Q. crispula[2], *A. sachalinensis*[2]	44°20′ N	142°15′ E	1949–1998	C	9	Tem	Nakatsuka *et al.* (2004)
Quercus lobata[2]	34°09′ N	118°44′ W	1791–1989	C	1	Cha	Feng & Epstein (1995)
Quercus petraea[2], *P. sylvestris*[1]	46°21′ N	8°36′ E	1600–2000	C	8	Tem	Reynolds-Henne *et al.* (2007)
Quercus robur[2]	52°50′ N	0°30′ E	1946–2000	C	2	Tem	Loader *et al.* (2003)
Quercus robur[2]	48°01′ N	02°10′ W	1909–1998	C	10	Tem	Masson-Delmotte *et al.* (2005)
Quercus robur[2]	48°20′ N	01° 50′ W	1880–1997	C	4	Tem	Raffalli-Delerce *et al.* (2004)
Q. robur[2], *P. sylvestris*[1]	50°03′N	20°20′E	1900–2003	C	4	Tem	Szczepanek *et al.* (2006)
Quercus rubra[2]	46°35′ N	79°40′ W	1918–1999	C	1	Tem	Bukata & Kyser (2007)
Quercus rubra[2]	44°58′ N	76°32′ W	1892–2000	C	1	Tem	Bukata & Kyser (2007)
Quercus rubra[2]	43°17′ N	79°48′ W	1884–2000	C	3	Tem	Bukata & Kyser (2007)
Quercus rubra[2]	44°37′ N	78°30′ W	1884–2000	C	1	Tem	Bukata & Kyser (2007)
Q. rubra[2], *P. sylvestris*[1]	52° N	0°30′ W	1895–1995	C	20	Tem	Hemming *et al.* (1998)
Quercus[2] *spp*	52°23′ N	20°42′ E	1700–1968	C	>20	Tem	Jedrysek *et al.* (2002)
Sabina przewalskii[1]	38°36′ N	99°52′ E	1948–1998	B	8	Tem	Zhang *et al.* (2007)
Swietenia macrophylla[2]	10°09′ S	59°26′ W	1875–1995	C	16	Rai	Hietz *et al.* (2005)

Table 1 (continued)

Tree species	Lat	Lon	Int	Sou	N	Bio	Ref
Taxodium ascendens[1]	25°16′ N	80°24′ W	1970–2000	C	4	Tem	Anderson *et al*. (2005)
Taxodium distichum[1]	26°54′ N	80°04′ W	1830–1990	C	3	Tem	Anderson *et al*. (2005)
Widdringtonia cedarbergensis[1]	32°24′ S	19°13′ E	1900–1977	C	32	Cha	February & Stock (1999)

in the atmospheric isotope ratio are considered, and the $^{13}C/^{12}C$ ratio in plant material is expressed as photosynthetic ^{13}C discrimination ($\Delta^{13}C$):

$$\Delta^{13}C = \frac{\delta^{13}C_a - \delta^{13}C_p}{1 + \delta^{13}C_p/1000} \quad (2)$$

where $\delta^{13}C_a$ and $\delta^{13}C_p$ are the respective isotopic ratios of atmospheric CO_2 and of plant material.

Based on a simplified Farquhar equation (Farquhar *et al*., 1989) carbon discrimination can be expressed as:

$$\Delta^{13}C = a + (b - a)\frac{C_i}{C_a} \quad (3)$$

where a is the $^{13}CO_2$ fractionation as a result of diffusion through air (4.4‰), b is the fractionation during carboxylation (27‰) by the CO_2-fixing enzyme Rubisco, C_i is the CO_2 concentration in leaf intercellular spaces, and C_a is the CO_2 concentration in the ambient air.

Consequently, C_i depends on CO_2 flux into the leaf, which is largely regulated by stomatal conductance, and CO_2 flux removed from the leaf for carbon fixation by assimilation. The intrinsic water-use efficiency (*iWUE*) is defined as the ratio between carbon assimilation (A) and stomatal conductance to water vapor (g_w):

$$iWUE = \frac{A}{g_w} \quad (4)$$

where A can be expressed as:

$$A = g_c(C_a - C_i) \quad (5)$$

in which g_c is the stomatal conductance to CO_2.

Substituting (5) in (4) and rearranging we obtain:

$$iWUE = \frac{g_c}{g_w}C_a\left(1 - \frac{C_i}{C_a}\right) = 0.625\ C_a\left(1 - \frac{C_i}{C_a}\right) \quad (6)$$

where 0.625 is the ratio between the stomatal conductance to CO_2, and the stomatal conductance to water vapor.

The simplified model of carbon discrimination, which neglects leaf internal conductances, can be problematic for the correct estimate of *iWUE*, as showed by Seibt *et al*. (2008). However, it is worthy to note that in this study the main focus was not on the actual value of *iWUE* but on the relationship between *iWUE*, atmospheric and climatic factors. Nevertheless, we evaluated the model effects due to uncertainty in *iWUE* (S1 supporting text).

From equation (3):

$$\frac{C_i}{C_a} = \frac{\Delta^{13}C - a}{b - a} \quad (7a)$$

$$C_i = C_a\frac{\Delta^{13}C - a}{b - a} \quad (7b)$$

Substituting (7a) in (6) we obtain an expression for the intrinsic water-use efficiency as a function of carbon isotope discrimination:

$$iWUE = 0.625\ C_a\left(1 - \frac{\Delta^{13}C - a}{b - a}\right) \quad (8)$$

Therefore, *iWUE* can be estimated from the carbon isotope ratio in tree rings ($\delta^{13}C_p$) taking into account the long-term variation in atmospheric CO_2 concentration (C_a) and its isotopic ratio ($\delta^{13}C_a$).

Variation in carbon isotopic discrimination and iWUE in response to rising atmospheric CO_2

Temporal variation in carbon isotope discrimination in response to the rising atmospheric CO_2 concentration was analyzed from 1850–2000, using three response scenarios proposed by Saurer *et al*. (2004) as a reference.

Scenario 1. The difference between CO_2 concentration in the air (C_a) and in leaf intercellular spaces (C_i) remains constant, therefore:

$$C_a - C_i = k \quad (9)$$

where k is a positive constant. Therefore, from equation (3):

$$\Delta^{13}C = a + (b - a)\frac{C_a - k}{C_a} \quad (10)$$

Under this scenario, for every C_a increase an equal increment in C_i is expected (constant stomatal drawdown), implying no changes in A and g_w or their proportional regulation. Under these conditions, we expect the greatest $\Delta^{13}C$ increase in response to rising CO_2, and no variation in intrinsic water-use efficiency (*iWUE* = 0.625 k).

In our calculations, we estimated k as the difference between the average atmospheric CO_2 concentration at the beginning of the industrial period (C_{a1850}), obtained as an average 1850–1870 value provided by McCarroll & Loader (2004), and an average, over the same period, of intercellular leaf concentration (C_{i1850}) values estimated from equation 7b; k was calculated separately for angiosperm and conifer species. The initial carbon isotope discrimination ($\Delta^{13}C_{1850}$) value was calculated as follows:

$$\Delta^{13}C_{a1850} = a + (b - a)\frac{C_{a1850} - k}{C_{a1850}} = b - \frac{(b - a)k}{C_{a1850}} \quad (11)$$

Under this assumption, we expect an increase in $\Delta^{13}C$ with time as a response to rising atmospheric CO_2 concentration (since $b > a$).

Scenario 2. It is hypothesized that trees make physiological adjustments to maintain a constant C_i/C_a ratio under rising atmospheric CO_2 concentration. This translates to a constant $\Delta^{13}C$ over time, and according to Eq. (6), suggests an increase in *iWUE* with rising C_a. An increase in intrinsic water-use efficiency can be the result of decreased stomatal conductance (g_w), or an increased rate of CO_2 assimilation (A), or both. In our calculations for this scenario we assumed a constant C_i/C_a ratio at the 1850 value.

Scenario 3. If the intercellular CO_2 concentration (C_i) is assumed constant, it results in $\Delta^{13}C$ decline over time under rising atmospheric CO_2 concentration. This indicates a greater increase in *iWUE* than in scenario 2. In this scenario C_i was set to its value in year 1850.

Predicting the effects of nitrogen deposition and climate

Generalized additive models (*GAMs*) were applied to inspect the shape of $\Delta^{13}C$ and *iWUE* response curves to the environmental predictor variables. *GAMs* are nonlinear and nonparametric regression techniques that do not require *a priori* functional relationship specifications between dependent and independent variables. The model strengths are the production of link functions to establish a relationship between the response variable mean and a smoothed function of each explanatory variable (Hastie & Tibshirani, 1990). A random effect was included in the model to account for variation among trees of the model intercept.

We successively predicted N deposition, CO_2, and climate effects on $\Delta^{13}C$ and *iWUE* by fitting a linear mixed-effect model, with a single level of grouping, to the data for 1950–2000. $\Delta^{13}C$ and *iWUE* were used alternatively as dependent variables, and data of angiosperm and conifer species were analyzed separately. As $\Delta^{13}C$ values, determined on annual tree rings, can be considered as repeated measures on the same individual chronology, we used the single chronology ($Chro_{ID}$) as grouping factor, based on the procedure described by Pinheiro & Bates (2000). The explanatory variables were annual values of atmospheric CO_2 concentration (C_a), nitrogen deposition rate (N_{rate}) or cumulative nitrogen deposition from 1950 to a specific year (N_{cum}), mean annual temperature (T_m), total annual precipitation (P), and number of wet days in a year (D_w). All explanatory variables were centered, as suggested by Schielzeth (2010), to avoid collinearity between main effects and their interaction. The dependent variable *iWUE* was *log*-transformed, and residuals were checked for normality, homoscedasticity and auto-correlation.

The tested model can be described as:

$$y_i = X_i\beta + Z_i b_i + \varepsilon_i \quad (12)$$

where β is the p-dimensional unknown vector of fixed effects (i.e. C_a, N_{rate} or N_{cum}, T_m, P, D_w), b_i is the q-dimensional unknown vector of random effects (i.e. $Chro_{ID}$), X_i and Z_i are, respectively, fixed and random effects regressor matrices, ε_i is the within group error vector. Both b_i and ε_i are assumed to have Gaussian distribution, i.e.

$$b_i = N \approx (0, \Sigma)$$

and

$$\varepsilon_i N \approx (0, \sigma^2)$$

Sites and time (years) were not explicitly considered as source of variation in the model. Differences among individual sites and through time were accounted for by environmental factors variability.

Maximum Likelihood (*ML*) and Restricted Maximum Likelihood (*RML*) estimates of random effects allowed estimates of intercept and slopes of regression parameters variability among different trees without "wasting" many degrees of freedom (i.e. only one parameter is computed overall to estimate the slope variance among different trees, instead of computing one slope for every tree). It is noteworthy that $Chro_{ID}$ encompasses among species variability in regression coefficients.

We began with a complex model that included all explanatory variables, variable interactions and quadratic terms. The model was subsequently simplified, and terms were individually deleted if the simpler model did not have significantly less explanatory power than the more complex one. The significance of each term was tested using a Likelihood Ratio Test (*LRT*). The ratios between the likelihoods between the more complex and simpler model were tested using a χ^2 as a reference distribution with degrees of freedom equal to the difference in number of parameters between the two models. *LRT* ratio test is frequently anticonservative (Pinheiro & Bates, 2000), i.e. it tends to underestimate the true P-value, therefore a parametric bootstrap approach was also used to test the dropped term significance whenever the P-value was between 0.2 and 0.001. At the end of the process, the final model showed lower AIC (Akaike Information Criterion) and BIC (Bayesian Information Criterion) values with respect to all previous and more complicated tested model permutations.

The model included a term that explicitly accounts for possible residual autocorrelations. The *ML* procedure was employed to compare and select among models with different fixed structures. At the end of the selection, the less biased REML procedure was applied to estimate model coefficients. Marginal testing of regression coefficients was used to estimate the significance of the effects of an explanatory variable after all other explanatory variables entered the model (for example the effect of C_a was estimated after N_{rate} or N_{cum}, T_m, P, D_w entered the model; or the effect of N_{rate} or N_{cum} was estimated after C_a, T_m, P, D_w entered the model). The possibility of separating the effect of different variables (*e.g.* nitrogen deposition from C_a or climatic variables) derived from interpreting the partial regression coefficient i.e. the amount by which the dependent variable was increased when one explanatory variable was increased by one unit, and the remaining explanatory variables were held constant.

We evaluated the model effects of uncertainty in within-cell N deposition. On the basis of the gridded map reported by Dentener *et al*. (2006), their Fig. 7, showing the standard deviation (SD) of N deposition in each grid, we ran the model 1000x, sampling a conservative random flat distribution around the mean (±1 SD; SD = 30% of the mean in each grid,

although we recognize this random variance may not fully account for the actual level of within-grid variability in some circumstances), and evaluated the effects on model coefficients.

All statistics and simulations were performed using the R statistical suite (R Development Core Team, 2011) using the '*nmle*' (linear mixed-effect models) and the '*mgcv*' (*GAMs* models) libraries.

Results

Nitrogen deposition and climatic variables

Atmospheric N deposition increased markedly at most of selected sites, particularly between 1950 and 1980 (Fig. 1). This reflects a general N deposition increase in the second half of the 20th century due to increasing emissions of nitrogen oxides (NO_x), most notably from fossil-fuel burning, and ammonia (NH_3) from agricultural activities. A global comparison of the underlying emission datasets with more recent emission estimates, and a discussion of uncertainty, is presented *e.g.* in Lamarque *et al.* (2010). At most sites outside Europe and North America, the calculated increase in N deposition continues into the 1990s, particularly in Asia. In many parts of Europe and North America, NO_x emissions have stabilized or decreased since ~1980 because of the implementation of air pollution policies. As a consequence, many North American sites analyzed in this study show stabilized N deposition in the 1980s or 1990s. At most European sites, N deposition stabilized or decreased in the 1980s.

For the year 2000, annual N deposition (N_{rate}) rates ranged from 0.06 to 1.84 g m^{-2} $year^{-1}$. The among sites variability in N_{rate} increased until 1970 and stabilized afterwards (Fig. 1). Cumulative N deposition (N_{cum}) was computed, for each calendar year, as total nitrogen deposition from 1950 to a selected year; and ranged from 2.1 to 85.7 g m^{-2} in the year 2000.

The correlation between climatic and atmospheric variables was generally weak, but in several cases is significant. The most relevant and significant ($P < 0.001$) correlations were as follows: between N_{rate} and P ($r = 0.33$), N_{rate} and D_w ($r = 0.36$), N_{rate} and C_a ($r = 0.34$); between N_{cum} and C_a ($r = 0.53$); and between D_w and P ($r = 0.63$), and D_w and T_m ($r = -0.26$ (Fig. S2).

Temporal trend of $\Delta^{13}C$ and iWUE

Results of the pooled data set (angiosperms and conifers together), and the entire period (1850–2000) showed a decreased carbon isotope ratio in woody rings ($\delta^{13}C_p$) by approximately 10 percent (from −22.1 to 24.3 ‰), and an increase of carbon discrimination ($\Delta^{13}C$) and intrinsic water-use efficiency (*iWUE*) by 4.6% (from 15.3 to 16.0 ‰) and 16.1% (from 90 to 105 mmol mol^{-1}), respectively. From 1950 to 2000, the

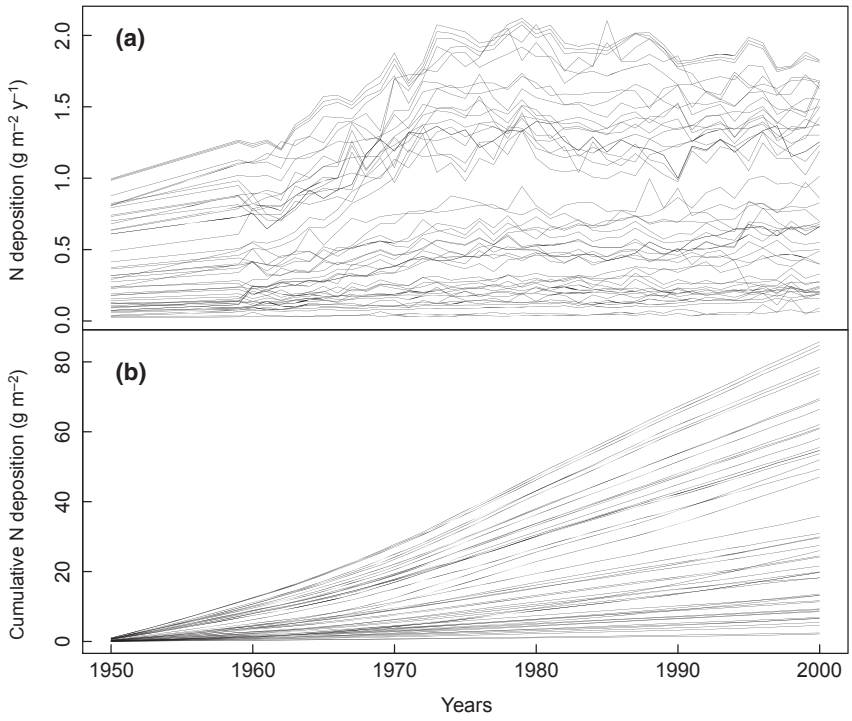

Fig. 1 Variation in annual N deposition rate (a) and cumulative N deposition (b) from1950–2000 at the selected sites.

rate of change for the same variables was 5.6%, 1.4% and 9.3%, respectively. Between 1850 and 2000, the greatest change in angiosperms vs. gymnosperms (26.4 vs. 22.9%) was in *iWUE*, and between 1950 and 2000 in conifers vs. angiosperms (18.4 vs. 12.7%); in our *iWUE* data set conifers exhibited a higher value than angiosperms (100 vs. 75 mmol mol^{-1} on average, between 1850 and 2000) (Table 2, Fig. S3).

Long-term variation in carbon isotope discrimination ($\Delta^{13}C$) was analyzed based on the three scenarios proposed by Saurer *et al.* (2004), and described in the previous section. The temporal patterns presented here were obtained by averaging data of each chronology for each calendar year from 1850–2000.

Temporal variation in $\Delta^{13}C$ was markedly different in angiosperm and conifer species. Since 1900 for angiosperms, most points were between *scenarios 2* and *3* with an apparent slightly declining trend (Fig. 2a). For conifer species, most points were between *scenarios 1* and *2* with a tendency, particularly in recent decades, to decrease towards a constant *scenario 2* value (Fig. 2b). For years 1950–2000, and for both angiosperms and conifers, *scenario 2* showed the lesser divergence from observed data in a Kolmogorov-Smirnov test, as it is also suggested by visual inspection of confidence intervals (Fig. 2). Rather similar results were observed when $\Delta^{13}C$ variation was represented as a function of atmospheric CO_2 concentration (Fig. S4).

The relationship between $\Delta^{13}C$ and time was further explored by fitting a linear random model, in which two random parameters accounted for the variance, among single chronologies ($Chro_{ID}$), of the slope and intercept of the linear model. BLUP (Best Linear Unbiased Prediction) estimates of slope frequency distribution of the $\Delta^{13}C$-year relationship showed some skewness, with asymmetry towards negative values for conifer and angiosperm species (Fig. 3).

We observed that, at least since 1900, C_a-C_i increased steadily as a function of time in angiosperm and in conifer species, with the steepest rise in conifers after 1950 (Fig. 4). The C_i/C_a ratio tended to remain constant, or showed a slight decrease over time (Fig. 5).

Assessing the effects of nitrogen deposition and climate

Generalized Additive Models (*GAMs*) were initially applied to explore the effect of predictor environmental variables on $\Delta^{13}C$ and on the intrinsic water-use efficiency estimated from single annual tree rings from 1950–2000. We used atmospheric CO_2 concentration, mean annual temperature, total annual precipitation and annual rate of N deposition (N_{rate}) or, alternatively, cumulative N deposition (N_{cum}) as covariates. Results indicated a weaker effect overall by N_{rate} (Fig. 6), however, independent analyses of the angiosperm and conifer data sets showed a linear and positive effect for CO_2 and N_{cum} (Fig. 7). Temperature exhibited no discernable effect in either data set, although a negative effect was detected by precipitation in only the conifer data set (Fig. S5).

Variation in *iWUE* and $\Delta^{13}C$ was further described by a linear mixed-effect model, including all covariates (C_a, T_m, P, D_w, N_{rate} or N_{cum}), their interactions, and quadratic terms. Beginning with a complex model, we

Table 2 Average values (±1 standard error) of $\delta^{13}C$ (‰), $\Delta^{13}C$ (‰) and *iWUE* (mmol mol^{-1}) over different periods between 1850 and 2000; observation numbers indicated in brackets

	Conifer species	*Angiosperm species*	*All species*
$\delta^{13}C$ (1850–1870)	−20.89 ± 0.17 (N = 62)	−24.07 ± 0.23 (N = 39)	−22.12 ± 0.21 (N = 101)
$\delta^{13}C$ (1950–1955)	−22.15 ± 0.12 (N = 135)	−24.40 ± 0.14 (N = 88)	−23.04 ± 0.12 (N = 223)
$\delta^{13}C$ (1980–2000)	−22.49 ± 0.20 (N = 48)	−25.39 ± 0.17 (N = 85)	−24.34 ± 0.18 (N = 133)
$\Delta^{13}C$ (1850–1870)	14.14 ± 0.16 (N = 62)	17.19 ± 0.22 (N = 39)	15.32 ± 0.20 (N = 101)
$\Delta^{13}C$ (1950–1955)	14.95 ± 0.11 (N = 135)	17.12 ± 0.13 (N = 88)	15.81 ± 0.11 (N = 223)
$\Delta^{13}C$ (1980–2000)	14.26 ± 0.19 (N = 48)	17.03 ± 0.16 (N = 85)	16.03 ± 0.17 (N = 133)
iWUE (1850–1870)	100.02 ± 1.35 (N = 62)	74.91 ± 1.85 (N = 39)	90.32 ± 1.64 (N = 101)
iWUE (1980–1955)	103.79 ± 1.05 (N = 135)	84.04 ± 1.12 (N = 88)	95.99 ± 1.02 (N = 223)
iWUE (1995–2000)	122.91 ± 1.53 (N = 48)	94.68 ± 1.67 (N = 85)	104.87 ± 1.74 (N = 133)
Percent change (%) 1850–2000			
$\delta^{13}C$	7.7	5.5	10.0
$\Delta^{13}C$	0.8	−0.9	4.6
iWUE	22.9	26.4	16.1
Percent change (%) 1950–2000			
$\delta^{13}C$	1.5	4.1	5.6
$\Delta^{13}C$	−4.6	−0.5	1.4
iWUE	18.4	12.7	9.3

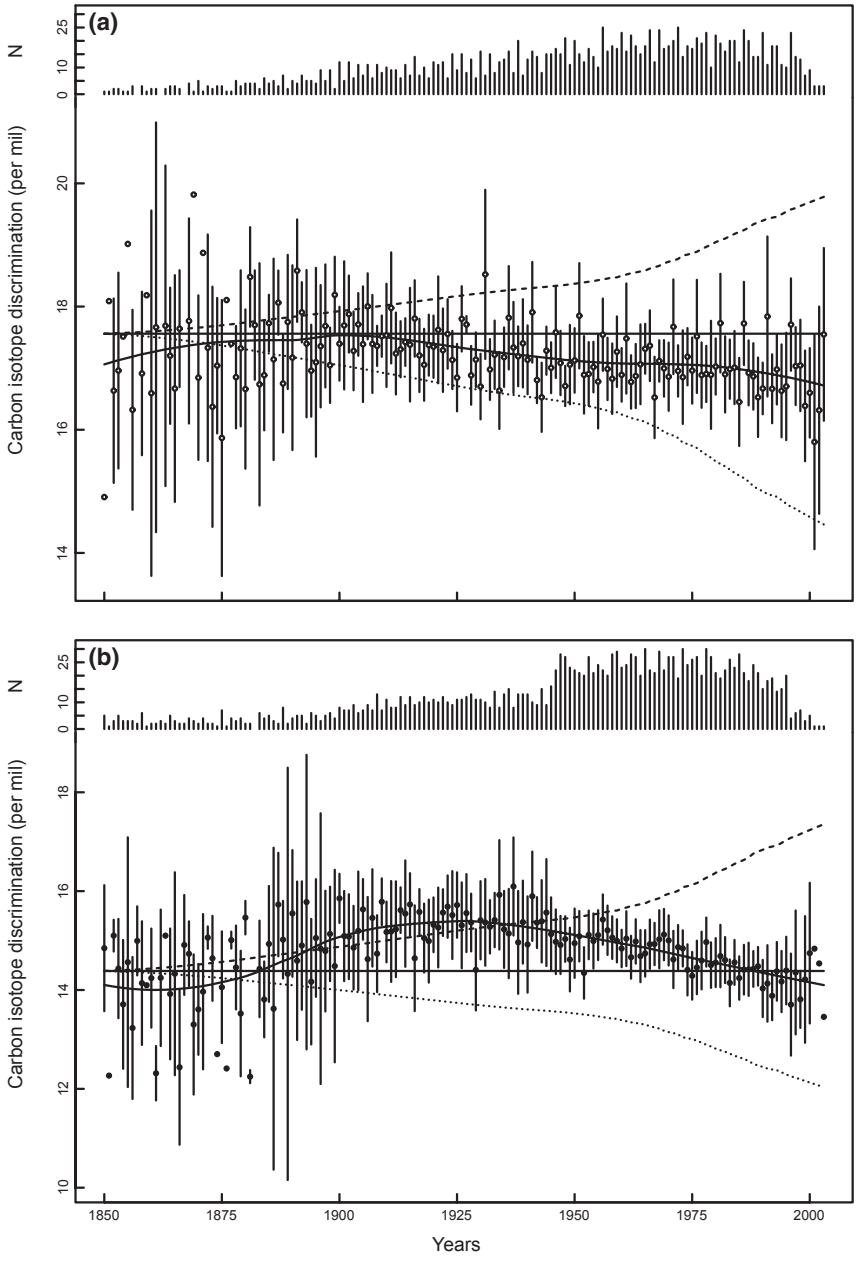

Fig. 2 Variation in carbon isotope discrimination ($\Delta^{13}C$) over the industrialization period (1850–2000) for angiosperm (a) and conifer (b) species. Lines represent hypothetical changes in $\Delta^{13}C$ due to increased atmospheric CO_2 concentrations (C_a) based on the three scenarios proposed by Saurer *et al*. (2004): a totally passive response (*scenario 1*, dashed line), a constant ratio between intercellular (C_i) and atmospheric CO_2 concentration (*scenario 2*, horizontal straight line), a constant C_i (*scenario 3*, dotted line). The continuous line corresponds to a locally weighed polynomial regression. Each point represents the mean of all tree chronologies of the corresponding species for a given year; vertical bars represent ± 1.96 SE. In the upper part of each panel, the number (N) of trees is reported.

progressively simplified the model following the procedure described in the methods. At the end of the selection process, the predictive models remained quite complex, with several significant interactions for angiosperms, and even more for the conifers. The model structures, the covariates with model coefficients, standard errors, and significance levels are summarized in Table 3 (N deposition included in the model as N_{rate}) and in Table 4 (N deposition included in the model as N_{cum}).

When N deposition was included in the model as annual deposition rate (N_{rate}), we observed a significant linear effect on *iWUE* and $\Delta^{13}C$ in conifer species, and a significant effect for the quadratic term of N_{rate} in the

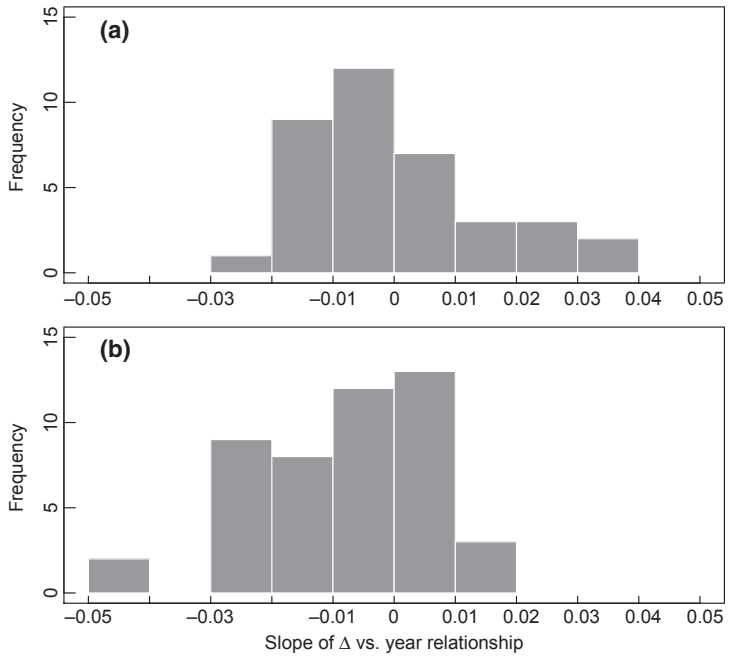

Fig. 3 Frequency distribution of carbon isotope discrimination ($\Delta^{13}C$) trend for angiosperm (a) and conifer species (b). Slopes are best linear unbiased predictions by a random model, where $\Delta^{13}C$ has been linearly regressed as a function of time. Random parameters accounted for among tree chronologies variances for the slope and the intercept of the linear model; the *y*-axis represents number of tree chronologies. Years were centered at A.D. 1850.

angiosperm data. Consequently, in angiosperms, CO_2 concentration appeared the most significant factor affecting *iWUE* within the range of our observations, and in conifers T_m, P, and D_w also exerted significant effects, as independent terms or interactions (Table 3).

Inclusion of N_{cum} in the model can result in a multicollinearity problem, as N_{cum} and C_a were significantly correlated in the data set ($r = 0.53$, $P < 0.01$, Fig. S2). This can affect the individual predictors coefficients and determination of the predictor producing the effect on the response variable can be a challenge. Therefore, the variance inflation factor (*VIF*) was applied to evaluate if multicollinearity was a threat to our model. Results showed the N_{cum} linear term in the model *VIF* was 4.6 for the angiosperm data set, and 3.5 for the conifer data set, suggesting low threat. Collinearity was primarily a problem for the quadratic terms and interactions.

Model results (Table 4) for angiosperms indicated N_{cum} was the only independent term with a significant positive effect on *iWUE*, however, a multi-factorial control was evident in conifers. In angiosperms, N_{cum} and C_a significantly affected $\Delta^{13}C$, and T_m and P were significant covariates in conifers (Table 4).

Overall, our final best models that described the $\Delta^{13}C$ and *iWUE* responses to predictor variables performed well in terms of goodness of fit for the angiosperm and conifer data sets (Fig. 8 and Fig. 9).

The model was robust for the effects of within-cell N deposition uncertainty. We performed 1000 simulations using N deposition values sampled randomly around the mean in each grid cell, resulting in the same model coefficients for N_{rate} as in Table 3: in the angiosperms, the quadratic N_{rate} term was significant in 999 of 1000 random simulations, the linear N_{rate} term was never significant; in the conifer data set, the linear N_{rate} term was significant in 1000 of 1000 random simulations; the term $C_a \times T_m \times N_{rate}$ was significant in 1000 of 1000 random simulations; the term $C_a \times T_m \times P \times N_{rate}$ was significant in 1000 of 1000 random simulations; and the term $C_a \times N_{rate}$ was significant in 603 of 1000 random simulations.

Discussion

Temporal trends of carbon discrimination and intrinsic water-use efficiency

The variation in carbon isotope discrimination ($\Delta^{13}C$) over the onset, progression and continued industrialization in a range of tree species and environmental conditions was characterized in this study.

Overall patterns suggested a change in $\Delta^{13}C$ under increased ambient CO_2, in angiosperm and conifer data set. This $\Delta^{13}C$ variation may reflect the capacity of trees to actively adjust leaf gas-exchange in conjunction with

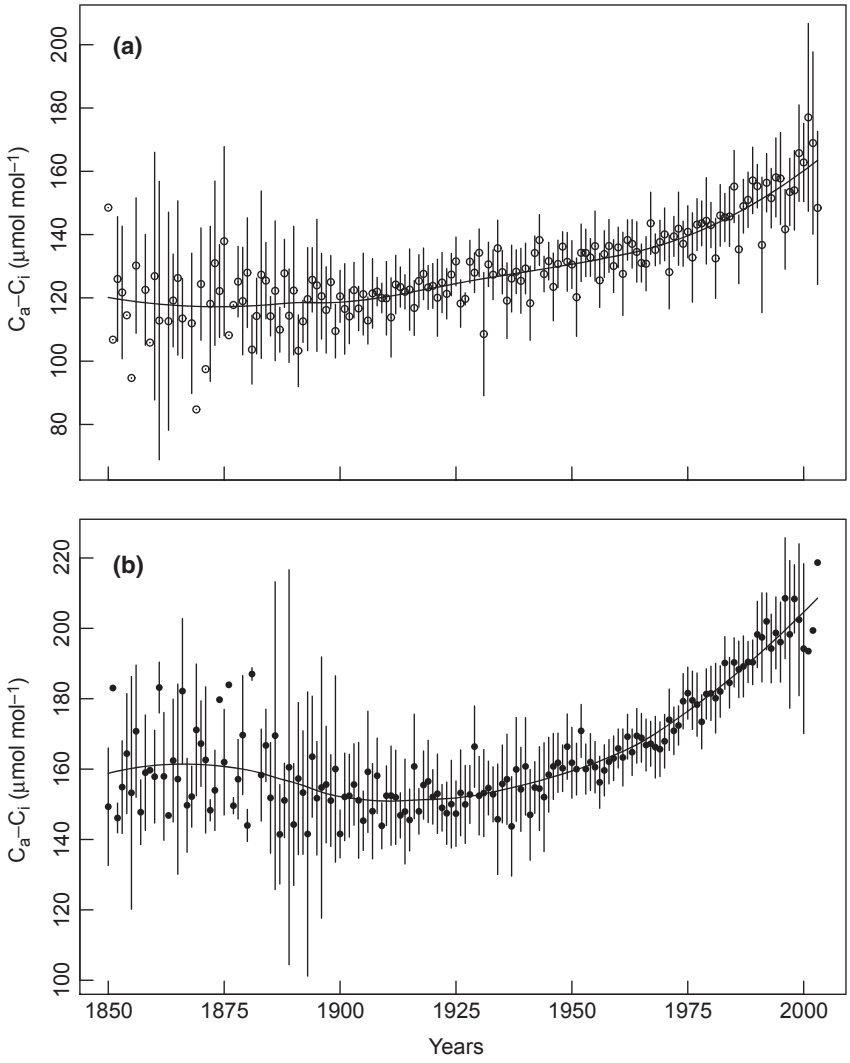

Fig. 4 Variation in the difference between atmospheric and intercellular CO_2 concentration from the 1850–2000 industrial period for angiosperm (a) and conifer (b) species. Each point indicates the mean of all tree chronologies of the corresponding species for a specific year; vertical bars represent ± 1.96 SE; the continuous line represents a locally weighed polynomial regression.

increasing CO_2 concentration. Indeed, by testing $\Delta^{13}C$ variation under idealized responses to increased ambient CO_2 (Saurer *et al*., 2004), *scenario 2* (constant C_i/C_a ratio) was nearer to observed data. Therefore, our results support the hypothesis of an active maintenance mechanism for a C_i/C_a constant (Ehleringer & Cerling, 1995), with associated increased *iWUE*, and are consistent with previous studies based on isotopic records from tree rings, that have generally revealed increased *iWUE* during analogous temporal periods for individual sites (e.g. Peñuelas & Azcón-Bieto, 1992; Feng & Epstein, 1995; Bert *et al*., 1997; Duquesnay *et al*., 1998; Feng, 1999; Saurer *et al*., 2004; Peñuelas *et al*., 2008; Peñuelas *et al*., 2011). Departure from response type could be an exception, and interpreted in terms of higher vulnerability to climate change, as suggested by Andreu-Hayles *et al*. (2011) for relic *Pinus uncinata* populations in Spain.

These patterns, observed for a wide range of species under different environmental conditions, provide further support to the observation that temporal change in $^{13}C/^{12}C$ ratios is only partly explained by changes in the isotopic ratio of atmospheric CO_2 ($\delta^{13}C_a$); this change can also be explained as an active response to the global rise in atmospheric CO_2 concentrations, which can involve both physiological and structural stomatal adaptations (De Boer *et al*., 2011).

The apparent trends of $\Delta^{13}C$ decline in the angiosperm and conifer data sets reinforce reports that climatic reconstructions using calibrated tree-ring isotope records can be biased if the response to varying ambient CO_2 concentrations was not properly addressed

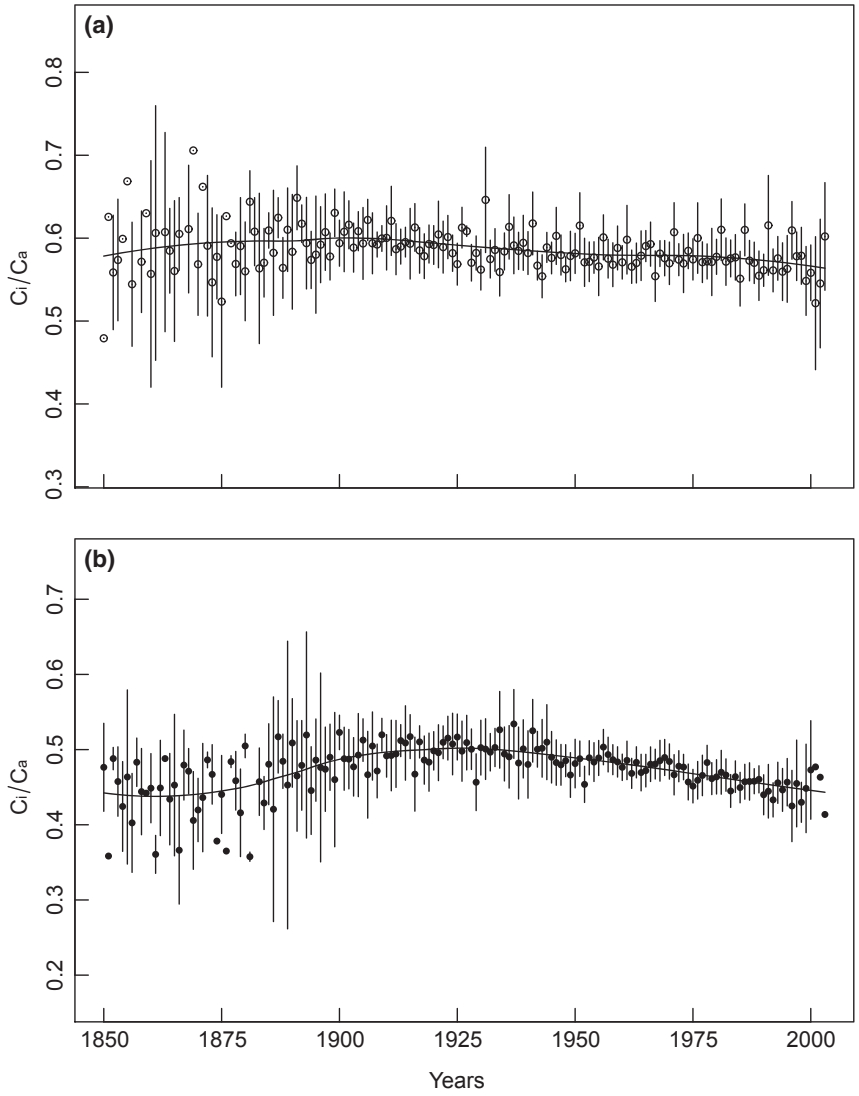

Fig. 5 Variation of the ratio between CO_2 concentration in leaf intercellular spaces (C_i) and the atmosphere (C_a) from 1850–2000 for angiosperm (a) and conifer (b) species. Each point indicates the mean of all tree chronologies of the corresponding species for a specific year; vertical bars represent ± 1.96 SE; the continuous line represents a locally weighed polynomial regression.

(McCarroll *et al.*, 2009). Quite surprisingly, this point remains neglected in studies that have applied quantitative $\Delta^{13}C$ patterns across environmental gradients to reconstruct past climatic conditions (Diefendorf *et al.*, 2010; Kohn, 2010).

Intrinsic water-use efficiency (*iWUE*) increased by 16.1% over the study period (1850–2000), and by 9.3% between 1950 and 2000. This is consistent with predictions from the majority of findings using isotopic tree-ring records (*e.g.* Feng & Epstein, 1995; Saurer *et al.*, 2004), and from results of a recent meta-analysis (Peñuelas *et al.*, 2011), where an increase of 20.5% was estimated for the second half of the last century. The increase in *iWUE* in conjunction with increased atmospheric CO_2 concentration is also congruent with models that predict a reduction in stomatal conductance, and structural adaptations in stomatal densities and pore sizes (De Boer *et al.*, 2011). In addition, a large body of evidence has been generated on elevated CO_2 effects on stomatal conductance and assimilation in short-term experiments, although the applicability of short-term responses to long-term physiological adjustments has been questioned (Körner, 2006). Enhanced *iWUE* may imply increased plant transpiration efficiency, and a positive effect on plant carbon balance. However, it has recently been shown that the increased *iWUE* observed during the last half century did not translate to increased tree growth (Peñuelas *et al.*, 2008; Andreu-Hayles *et al.*, 2011; Peñuelas *et al.*, 2011). Nonetheless, enhanced *iWUE* has the potential to aid trees

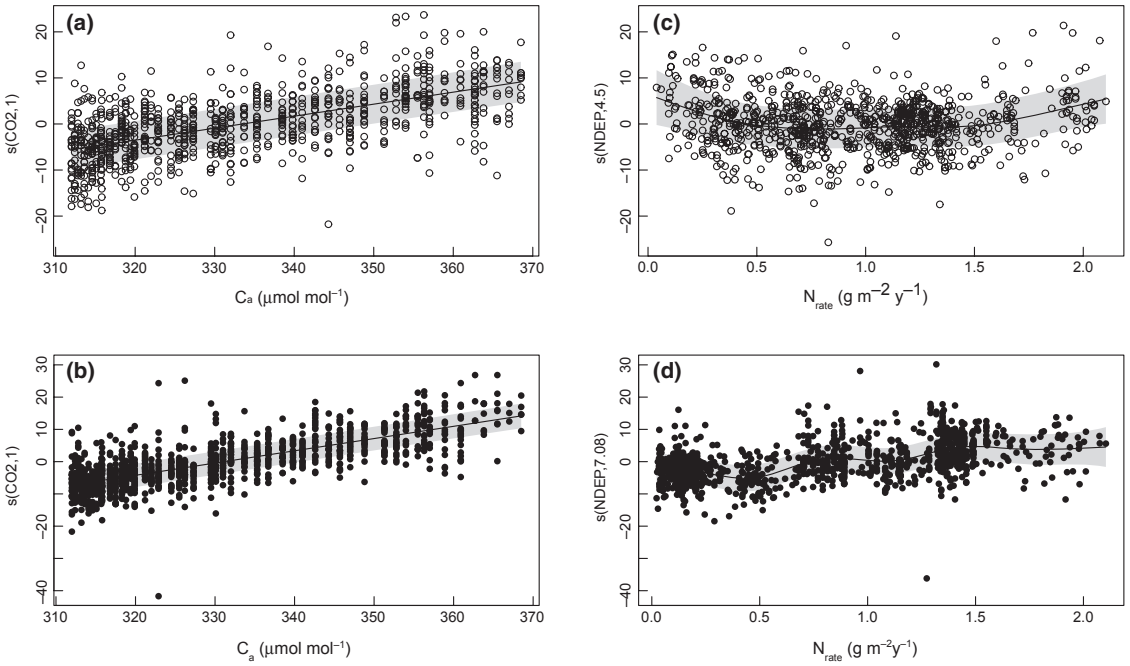

Fig. 6 Generalized Additive Modeling (GAM) results of atmospheric CO_2 concentration (C_a) effects, panels (a) and (b), and annual rate of N deposition (N_{rate}) effects, panels (c) and (d), on intrinsic water-use efficiency (*iWUE*). The *y*-axis values indicate the *x*-axis covariate effect on the iWUE deviation from the mean predicted by the model (continuous line). Symbols are partial residuals around predicted covariate effects; empty circles for angiosperms, panels (a) and (c); filled circles for conifers, panels (b) and (d). The shaded areas indicate the 95% confidence interval. The number on each *y*-axis caption is the effective degrees of freedom for the term being plotted.

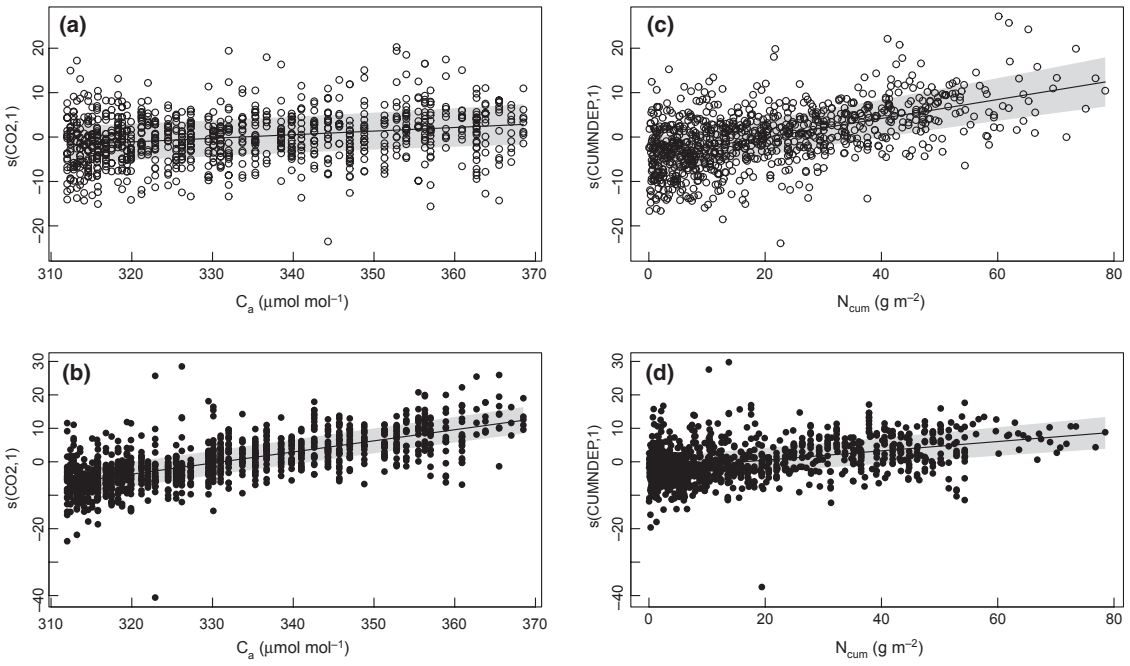

Fig. 7 Generalized Additive Modeling (GAM) results of atmospheric CO_2 concentration (C_a) effects, panels (a) and (b), and cumulative N deposition (N_{cum}) effects, panels (c) and (d), on intrinsic water-use efficiency (*iWUE*). The *y*-axis values indicate the *x*-axis covariate effect on the iWUE deviation from the mean predicted by the model (continuous line). Symbols are partial residuals around predicted covariate effects; empty circles for angiosperms, panels (a) and (c); filled circles for conifers, panels (b) and (d). The shaded areas indicate the 95% confidence interval. The number on each *y*-axis caption is the effective degrees of freedom for the term being plotted.

Table 3 Linear mixed-models. Coefficients (*Cf*) of predictor variables in selected linear mixed-models ($y_i = X_i\beta + Z_i b_i + \varepsilon_i$, see methods); $y = ln(iWUE)$ and $y = \Delta^{13}C$; C_a= ambient CO_2 concentration (μmol mol^{-1}); T_m = mean annual temperature (°C); P = total annual precipitation (mm); D_w = number of wet days; N_{rate} = annual rate of nitrogen deposition (g m^{-2} year^{-1})

	$y = ln\ (iWUE)$				$y = \Delta^{13}C$			
	Angiosperms (df = 877)		*Conifers (df = 1023)*		*Angiosperms (df = 827)*		*Conifers (df = 1015)*	
	Cf	*SE*	*Cf*	*SE*	*Cf*	*SE*	*Cf*	*SE*
Model intercept	4.4^{**}	$2.9\cdot10^{-3}$	4.7^{**}	$1.9\cdot10^{-2}$	17.3^{**}	$2.4\cdot10^{-1}$	14.8^{**}	$2\cdot10^{-1}$
C_a	$2.8\cdot10^{-3**}$	$0.5\cdot10^{-3}$	$2.6\cdot10^{-3**}$	$3\cdot10^{-4}$	$-4\cdot10^{-4}$	$4.5\cdot10^{-4}$	$3.6\cdot10^{-3}$	$3.8\cdot10^{-3}$
N_{rate}	$-1.3\cdot10^{-3}$	$2.2\cdot10^{-2}$	$6.9\cdot10^{-2**}$	$1.9\cdot10^{-2}$	$2.4\cdot10^{-1}$	$2.1\cdot10^{-4}$	$-7.5\cdot10^{-1*}$	$2.3\cdot10^{-1}$
T_m	$2.3\cdot10^{-3}$	$3.1\cdot10^{-3}$	$5\cdot10^{-3**}$	$1.9\cdot10^{-3}$	$-2.1\cdot10^{-2}$	$2.7\cdot10^{-2}$	$-6.7\cdot10^{-2**}$	$1.7\cdot10^{-2}$
P	$-2\cdot10^{-4}$	$-2\cdot10^{-4}$	$3\cdot10^{-5**}$	$0.7\cdot10^{-5}$	$1.9\cdot10^{-4}$	$1.6\cdot10^{-4}$	$3.6\cdot10^{-4**}$	$7\cdot10^{-5}$
D_w	$-3.6\cdot10^{-3}$	$2.4\cdot10^{-3}$	$-2.7\cdot10^{-2**}$	$1.3\cdot10^{-3}$	$1.9\cdot10^{-2}$	$2.0\cdot10^{-2}$	$2.6\cdot10^{-2}$	$1.5\cdot10^{-2}$
C_a^2	$-2\ 10^{-5*}$	$1\cdot10^{-5}$	$-0.7\cdot10^{-5}$	$0.1\cdot10^{-5}$	$1.7\cdot10^{-4}$	$1.6\cdot10^{-4}$	$3\cdot10^{-5}$	$1.5\cdot10^{-4}$
N_{rate}^2	$6.7\cdot10^{-2*}$	$2\cdot10^{-2}$	–		$-6.8\cdot10^{-1**}$	$2\cdot10^{-1}$	–	
T_m^2	–		$-3\cdot10^{-3*}$	$1\cdot10^{-4}$	–		$1.4\cdot10^{-3}$	$1.1\cdot10^{-3}$
$C_a \cdot T_m$	–		$-7\cdot10^{-5*}$	$3\cdot10^{-5}$	–		$1.1\cdot10^{-3*}$	$4.6\cdot10^{-4}$
$C_a \cdot P$	$-1\cdot10^{-6*}$	$0.5\cdot10^{-6}$	$-2\cdot10^{-6**}$	$4\cdot10^{-7}$	$1\cdot10^{-5*}$	$5\cdot10^{-6}$	$2\cdot10^{-5**}$	$5\cdot10^{-6}$
$C_a \cdot D_w$	–		$-2\cdot10^{-4**}$	$7\cdot10^{-5}$	–		$-2\cdot10^{-3**}$	$7.7\cdot10^{-4}$
$C_a \cdot N_{rate}$	–		$9\cdot10^{-4}$	$5\cdot10^{-4}$	–		$-1.1\cdot10^{-2}$	$9\cdot10^{-2}$
$T_m \cdot D_w$	$2.2\cdot10^{-3**}$	$0.4\cdot10^{-3}$	–		$-1.6\cdot10^{-2**}$	$4.2\cdot10^{-3}$	–	
$T_m \cdot N_{rate}$	$1\cdot10^{-5**}$	$0.3\cdot10^{-5}$	–		$-9\cdot10^{-2*}$	$3.8\cdot10^{-2}$	–	
$T_m \cdot P$	–		$5\cdot10^{-6**}$	$9\cdot10^{-7}$	–		$-5\cdot10^{-5**}$	$1\cdot10^{-5}$
$P \cdot N_{rate}$	–		$6\cdot10^{-5**}$	$1\cdot10^{-5}$	–		$-6.1\cdot10^{-4**}$	$1.4\cdot10^{-4}$
$P \cdot D_w$	–		–		$9.1\cdot10^{-5**}$	$2\cdot10^{-5}$	–	
$C_a \cdot T_m \cdot N_{rate}$	–		$-3\cdot10^{-4**}$	$7\cdot10^{-5}$	–		$4.8\cdot10^{-3**}$	$8.3\cdot10^{-4}$
$C_a \cdot T_m \cdot P \cdot N_{rate}$	–		$2\cdot10^{-7**}$	$5\cdot10^{-8}$	–		$3\cdot10^{-6**}$	$8\cdot10^{-7}$

* and ** denote statistical significance at $P < 0.05$ and $P < 0.01$, respectively.

during drought stress conditions associated with climate change (*e.g.* Giuggiola *et al.*, 2010), and to overcome other environmental growth limitations.

Our results showed no indication that the rate of increase of *iWUE* was reduced at higher ambient CO_2 values, rather in conifers it was higher in recent years (Fig. 4). Waterhouse *et al.* (2004) showed that *Pinus sylvestris* growing in Siberia experienced a reduction in *iWUE* sensitivity due to increasing C_a, and suggested this represented a saturation effect related to a loss in climatic sensitivity of latewood relative density. Alternatively, a modeling exercise performed on sub-tropical angiosperms and conifers suggested that structural changes could persist beyond doubled CO_2 levels with respect to current levels (De Boer *et al.*, 2011), with adaptations lasting longer and being more pronounced in conifers, as our data indicate.

The role of nitrogen deposition and climatic variables

This is the first reported study to describe large-scale spatial and temporal variation in $\Delta^{13}C$ and *iWUE* under rising CO_2 conditions that included nitrogen deposition among environmental predictors. Statistical modeling was conducted on individual tree ring records, which were affected by short-term fluctuations in $^{13}C/^{12}C$ ratios in relationship to year-to-year variations in climatic conditions, *e.g.* summer temperature, evaporative demand, and precipitation, among others (Berninger *et al.*, 2000; Waterhouse *et al.*, 2004). Furthermore, our data set incorporated relevant sources of variation, including differences across a broad species range, among and within species variability, and local climatic gridded simulated data conditions.

Overall, we were able to define statistical descriptive models that performed well in terms of goodness of fit (Fig. 8 and Fig. 9), exhibiting robust predictive power based on the covariate set for the angiosperm and conifer data sets.

No single predictor variable had a clearly predominant effect, however, $\Delta^{13}C$ and *iWUE* showed complex dependent interactions between different covariates, including nitrogen deposition. A significant linear effect of N_{rate} on *iWUE* and $\Delta^{13}C$ was observed in

Table 4 Coefficients (*Cf*) of predictor variables in selected linear mixed-models ($y_i = X_i\beta + Z_i b_i + \varepsilon_i$, see methods); $y = ln$ (*iWUE*) and $y = \Delta^{13}C$; C_a = ambient CO_2 concentration (μmol mol^{-1}); T_m = mean annual temperature (°C); P = total annual precipitation (mm); D_w = number of wet days; N_{cum} = cumulative nitrogen deposition to a given year (g m^{-2})

	$y = ln$ (*iWUE*)				$y = \Delta^{13}C$			
	Angiosperms (df = 879)		*Conifers (df = 1021)*		*Angiosperms (df = 830)*		*Conifers (df = 1013)*	
	Cf	*SE*	*Cf*	*SE*	*Cf*	*SE*	*Cf*	*SE*
Model intercept	4.4^{**}	$2.7\cdot10^{-3}$	4.7^{**}	$1.7\cdot10^{-2}$	17.3^{**}	$2.2\cdot10^{-1}$	14.8^{**}	$1.9\cdot10^{-1}$
C_a	$7\cdot10^{-4}$	$8\cdot10^{-4}$	$1.2\cdot10^{-3*}$	$6\cdot10^{-4}$	$1.7\cdot10^{-2*}$	$6.9\cdot10^{-3}$	$2.2\cdot10^{-2**}$	$6.8\cdot10^{-3}$
N_{cum}	$2.2\cdot10^{-3*}$	$9\cdot10^{-4}$	$2.8\cdot10^{-3**}$	$7\cdot10^{-4}$	$-1.7\cdot10^{-1*}$	$7.4\cdot10^{-3}$	$-3.1\cdot10^{-2*}$	$8.7\cdot10^{-3}$
T_m	$2.3\cdot10^{-3}$	$2.9\cdot10^{-3}$	$3.7\cdot10^{-3*}$	$1.5\cdot10^{-3}$	$-3.3\cdot10^{-2}$	$2.7\cdot10^{-2}$	$-5.7\cdot10^{-2**}$	$1.7\cdot10^{-2}$
P	$-2\cdot10^{-5}$	$2\cdot10^{-5}$	$-2\cdot10^{-5*}$	$7\cdot10^{-6}$	$2\cdot10^{-4}$	$2\cdot10^{-4}$	$2\cdot10^{-4*}$	$7\cdot10^{-5}$
D_w	$-1.4\cdot10^{-3}$	$2.2\cdot10^{-3}$	$-2.8\cdot10^{-3*}$	$1.3\cdot10^{-3}$	$1.4\cdot10^{-2}$	$2.0\cdot10^{-2}$	$2.6\cdot10^{-2}$	$1.5\cdot10^{-2}$
C_a^2	–		–		–		–	–
N_{cum}^2	–		–		–		$-7\cdot10^{-4}$	$4\cdot10^{-4}$
T_m^2	–		$-3\cdot10^{-3*}$	$1\cdot10^{-4}$	–			
$C_a \cdot T_m$	–		–		–			
$C_a \cdot P$	$-1\cdot10^{-6*}$	$5\cdot10^{-7}$	$-3\cdot10^{-6**}$	$6\cdot10^{-7}$	$1\cdot10^{-5*}$	$5\cdot10^{-6}$	$3\cdot10^{-5**}$	$7\cdot10^{-6}$
$C_a \cdot D_w$	–		$-2\cdot10^{-4*}$	$7\cdot10^{-5}$	–		$-2.2\cdot10^{-3**}$	$7\cdot10^{-4}$
$C_a \cdot N_{cum}$	–		$8\cdot10^{-5*}$	$4\cdot10^{-5}$	–		$1.2\cdot10^{-3**}$	$4\cdot10^{-4}$
$T_m \cdot D_w$	$1.5\cdot10^{-3**}$	$4\cdot10^{-4}$	–		$-1.5\cdot10^{-2**}$	$4.1\cdot10^{-3}$	–	
$P \cdot N_{cum}$	–		$3\cdot10^{-6**}$	$6\cdot10^{-7}$	–		$-3\cdot10^{-5**}$	
$T_m \cdot P$	–		$6\cdot10^{-6**}$	$1\cdot10^{-6}$	–		$-7\cdot10^{-5**}$	$7\cdot10^{-6}$
$P \cdot D_w$	$9\cdot10^{-6**}$	$3\cdot10^{-6}$	–		$-9.1\cdot10^{-5**}$	$2\cdot10^{-5}$	–	
$C_a \cdot T_m \cdot N_{cum}$	–		$-4\cdot10^{-6}$	$2\cdot10^{-6}$	–		$5\cdot10^{-5}$	$3\cdot10^{-5}$
$C_a \cdot T_m \cdot D_w$	–		$-3\cdot10^{-5**}$	$8.3\cdot10^{-6}$	–		$4\cdot10^{-4**}$	$9\cdot10^{-5}$
$C_a \cdot P \cdot N_{cum}$	–		$-4\cdot10^{-8*}$	$2\cdot10^{-8}$	–		$1\cdot10^{-6*}$	$2\cdot10^{-7}$
$T_m \cdot P \cdot N_{cum}$	–		$3\cdot10^{-7}$	$7.3\cdot10^{-8}$	–		$-3\cdot10^{-6**}$	$8\cdot10^{-7}$
$C_a \cdot T_m \cdot P \cdot N_{cum}$	–		$-6\cdot10^{-9}$	$4\cdot10^{-9}$	–		$3\cdot10^{-6}$	$4\cdot10^{-8}$
$C_a \cdot T_m \cdot D_w \cdot N_{cum}$	–		$-2\cdot10^{-6*}$	$7\cdot10^{-7}$	–		$2\cdot10^{-5**}$	$8\cdot10^{-7}$

* and ** denote statistical significance at $P < 0.05$ and $P < 0.01$, respectively; *SE*=standard error.

conifers, and the angiosperms showed a significant quadratic effect of N_{rate} (Table 3). These results were reflected in the GAM patterns that emerged, and offered an additional tool to ascertain the relationship nature between $\Delta^{13}C$ and *iWUE*, and the explanatory variable set (Fig. 6).

Among the climatic predictors, precipitation was the only variable to display a discernable negative effect on the conifer data set (Fig. S4). Given recent analyses of global carbon discrimination patterns across environmental conditions, which indicated dominant control of mean annual precipitation (Diefendorf *et al*., 2010), a multi-factorial environmental control on $\Delta^{13}C$ and *iWUE* was revealed in our analysis. The results suggested nitrogen deposition as a significant factor in the regulation of water loss-carbon gain balance at the leaf level.

We recognize the entire question may be more complicated if atmospheric changes, other than N deposition, are considered *e.g*., tropospheric ozone pollution and SO_x deposition, which frequently co-occur with N deposition. In the ozone, there is normally a positive correlation with N deposition because NO_x stimulates chemical production of O_3; for sulfur, the correlation strength depends on the component of interest (Lamarque *et al*., 2010). In our data set, O_3 and SO_x were positively and significantly correlated with N deposition, and both increased until the 1970s, and tended to stabilize afterward (Fig. S2 and Fig. S6).

Tropospheric ozone and SO_x affect leaf physiology, and frequently exert a negative effect on assimilation rate (Wittig *et al*., 2007, 2009, Guerrieri *et al*. 2011). We applied GAMs to our data set to assess the possible influence of these pollutants on *iWUE* using C_a, T_m, P, and alternatively O_3 and SO_x deposition values, as environmental predictors.

No clear pattern emerged from the angiosperm and conifer data sets (Fig. S7). We acknowledge this result does not rule out the hypothesis that the pollutants may interact with N deposition and affect *iWUE*. However, the physiological effects expected on *iWUE* by O_3 and SO_x are rather different from those expected by N deposition. In particular, the deposition of these pollutants

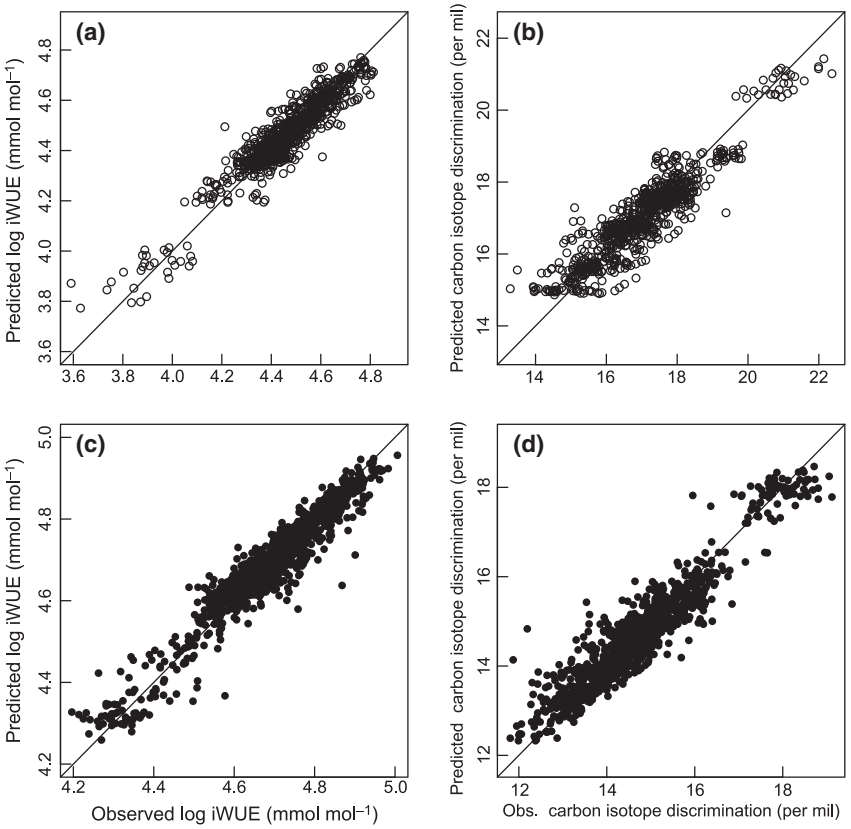

Fig. 8 Goodness of fit for the selected linear-mixed models (N deposition included as annual rate, N_{rate}) for intrinsic water-use efficiency (*iWUE*), panels (a) and (b), and carbon isotope discrimination ($\Delta^{13}C$), panels (c) and (d). Empty circles, panels (a) and (c) represent angiosperms, filled circles, panels (b) and (d) represent conifers; the solid line represents a 1 : 1 relationship.

may negate the potential beneficial N-deposition effects (Wittig *et al.*, 2009; Guerrieri *et al.*, 2011), making it difficult to argue that the patterns we observed were caused by sulfur or ozone deposition. In a simulation study, Ollinger *et al.* (2002) estimated that tropospheric ozone can offset a substantial proportion of the increased carbon sink driven by CO_2 and N deposition, which was supported by a more recent meta-analysis (Wittig *et al.*, 2009). Interestingly, Wittig *et al.* (2007) reported that conifers were significantly less sensitive than angiosperms to elevated O_3. An interactive ozone and N-deposition effect may be considered in the interpretation of the different *iWUE* to N_{rate} responses between conifers and angiosperms (Table 3, Fig. 6).

Our results were not sufficient to offer the causal mechanisms underlying *iWUE* response to N deposition. However, former studies have demonstrated nitrogen-deposition effects can arise as a consequence of the large fraction (up to 70%) of atmospheric nitrogen intercepted by tree crowns (Gaige *et al.*, 2007; Neirynck *et al.*, 2007; Sievering *et al.*, 2007), which accounts for a significant amount of tree nitrogen requirements (Harrison *et al.*, 2000). Sparks (2009) conducted a simulation study and found effective nitrogen compound capture by forest canopies, and direct canopy nitrogen uptake, which increased carbon storage capacity in forest ecosystems (Dezi *et al.*, 2010). To date, only a few field experiments including Deepsyke Forest, UK (Sheppard *et al.*, 2004, 2008,) and Howland Forest, USA (Gaige *et al.*, 2007; Dail *et al.*, 2009) have examined the effects of direct nitrogen spraying above the forest canopy. In a recent analysis of the Deepsyke experiment, Guerrieri *et al.* (2011) determined that canopy nitrogen applications increased tree *iWUE* with the magnitude of changes related to soil conditions, and the availability of other nutrients.

The multifactorial control highlighted by our analysis agrees with observations that N availability can interact with other environmental conditions in affecting carbon isotope discrimination and *iWUE*. For example, Högberg *et al.* (1993) observed a significant interaction between enhanced nitrogen availability over long-term fertilization experiments, and water stress on leaf $^{13}C/^{12}C$ ratio in conifers.

As stated before, the inclusion of N_{cum} in the model can result in multicollinearity. This is a quite common problem in ecological studies, and can lead to an

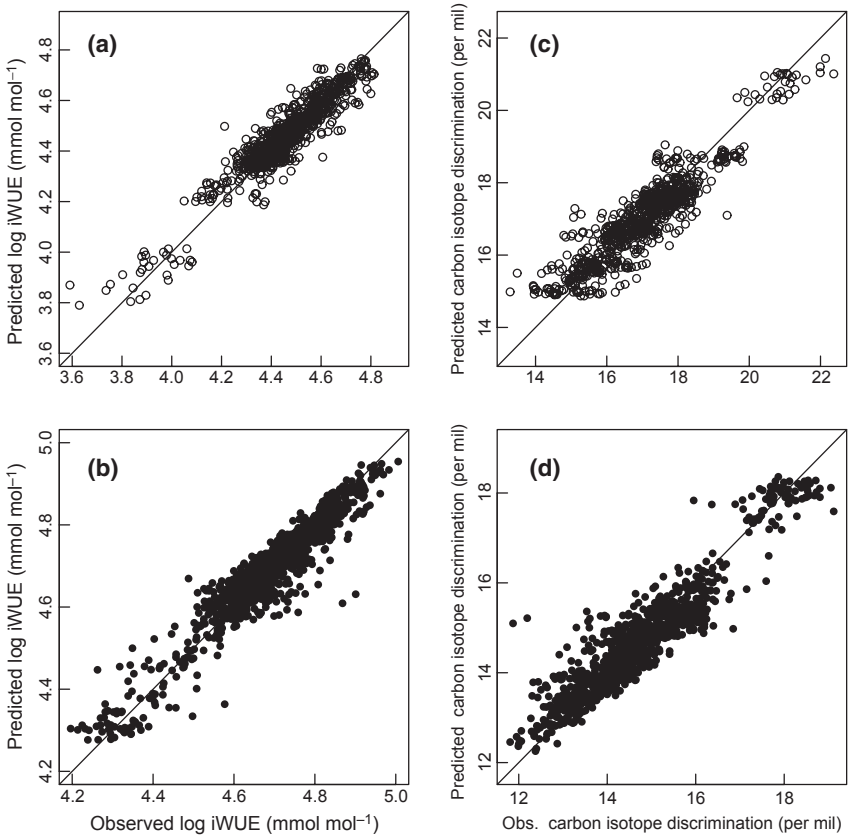

Fig. 9 Goodness of fit for the selected linear-mixed models (N deposition included as annual rate, N_{cum}) for intrinsic water-use efficiency (*iWUE*), panels (a) and (b), and carbon isotope discrimination ($\Delta^{13}C$), panels (c) and (d). Empty circles, panels (a) and (c) represent angiosperms, filled circles, panels (b) and (d) represent conifers; the solid line represents a 1 : 1 relationship.

incorrect exclusion of some variables during model selection, particularly when the effect of one variable is weaker with respect to other predictors (Graham, 2003). Based on Freckleton (2010), ordinary least square models usually yield unbiased parameter estimate irrespective of the degree of correlation of predictors.

We recognize that the reduction in the coefficients for C_a when N_{cum} is used rather than N_{rate} (compare Tables 3 and 4) does suggest that some of the effect of N_{cum} is accounted for by co-variance with C_a, however, a robust estimation of predictor coefficients was possible at least in the angiosperm data set, and indicated a significant and positive association of N_{cum} and *iWUE*. This result supports the hypothesis that long-term soil N accumulation may lead to enhanced plant nutritional status (Aber *et al*., 2003), which can stimulate photosynthesis and increase *iWUE*.

The following conclusions can be drawn from this study: *i*) given temporal variation in $\Delta^{13}C$ under potential extreme responses to increased ambient CO_2, our results support the hypothesis of an active plant mechanism that maintains a constant ratio between intercellular and ambient CO_2 concentrations; *ii*) we emphasize that climatic reconstructions using tree-ring isotope records can be biased if the response to varying ambient CO_2 concentrations is not adequately addressed; *iii*) intrinsic water-use efficiency increased over the study period, and no sign emerged that the *iWUE* rate increase was reduced at higher ambient CO_2 values; *iv*) linear mixed-effects models were effective to describe the variation in $\Delta^{13}C$ and *iWUE* as a function of a set of environmental predictors, including annual rate (N_{rate}) and long-term cumulative (N_{cum}) deposition; *v)* no single climatic or atmospheric variable had a clearly predominant effect, however, $\Delta^{13}C$ and *iWUE* showed complex dependent interactions between different covariates; and *vi)* a significant association of N_{rate} with *iWUE* and $\Delta^{13}C$ was observed in conifers and in the angiosperms, and in the angiosperms N_{cum} was the only independent term with a significant positive association with *iWUE*.

Acknowledgements

This research was jointly supported by MIUR-FISR "Carbo-Italy"and MIUR-PRIN projects awarded to M.B. Contributions by S.L. and T.G. were equally important.

The Ph.D. program "Crop systems, Forestry, and Environmental Sciences" (University of Basilicata, Italy) supported T.G; R.G. received funding from a Newton International Fellowship granted by the Royal Society, the British Academy, and the Royal Academy of Engineering. UK. M.M. acknowledges the contribution of NERC grant NE/G00725X/1 "Impacts of nitrogen deposition on the forest carbon cycle: from ecosystem manipulations to national scale predictions". We thank A. Nolè (University of Basilicata) for technical support. The valuable comments by three anonymous referees greatly contributed to improve the paper.

References

Van Aardenne JA, Dentener FJ, Olivier JGJ, Klein Goldewijk CGM, Lelieveld J (2001) A 1o x 1o resolution data set of historical anthropogenic trace gas emissions for the period 1890–1990. *Global Biogeochemical Cycles*, **15**, 909–928.

Aber JD, Goodale CL, Ollinger SV *et al.* (2003) Is nitrogen deposition altering the nitrogen status of northeastern forests? *BioScience*, **53**, 375–389.

Ainsworth S, Rogers A (2007) The response of photosynthesis and stomatal conductance to rising [CO_2]: mechanisms and environmental interactions. *Plant, Cell and Environment*, **30**, 252–270.

Anderson WT, Bernasconi SM, McKenzie JA (1998) Oxygen and carbon isotopic record of climatic variability in tree ring cellulose (Picea abies): an example from central Switzerland (1913–1995). *Journal of Geophysical Research*, **103**, 625–631.

Anderson WT, Sternberg LSL, Pinzon MC, Gann-Troxler T, Childersb DL, Duever M (2005) Carbon isotopic composition of cypress trees from South Florida and changing hydrologic conditions. *Dendrochronologia*, **23**, 1–10.

Andreu-Hayles L, Planell O, Gutiérrez E, Muntan E, Helle G, Anchukaitis KJ, Schleser GH (2011) Long tree-ring chronologies reveal 20th century increases in water-use efficiency but no enhancement of tree growth at five Iberian pine forests. *Global Change Biology*, **17**, 2095–2112.

Battipaglia G, Cherubini P, Saurer M, Siegwolf RTW, Strumia S, Cotrufo MF (2007) Volcanic explosive eruptions of the Vesuvio decrease tree-ring growth but not photosynthetic rates in the surrounding forests. *Global Change Biology*, **13**, 1–16.

Berninger F, Sonninen E, Aalto T, Lloyd J (2000) Modeling ^{13}C discrimination in tree rings. *Global Biogeochemical Cycles*, **1**, 213–223.

Bert D, Leavitt SW, Dupouey JL (1997) Variations of wood $\delta^{13}C$ and water-use efficiency of *Abies alba* during the last century. *Ecology*, **78**, 1588–1596.

De Boer HJ, Lammertsm EI, Wagner-Cremer F, Dilcher DL, Wassen MJ, Dekker SC (2011) Climate forcing due to optimization of maximal leaf conductance in subtropical vegetation under rising CO_2. *Proceedings of the National Academy of Sciences USA*, **108**, 4041–4046.

Bonan GB (2008) Forests and climate change: forcings, feedbacks, and the climate benefits of forests. *Science*, **320**, 1444–1449.

Brueck H (2008) Effects of nitrogen supply on water-use efficiency of higher plants. *Journal of Plant Nutrition and Soil Science*, **171**, 210–219.

Bukata AR, Kyser TK (2007) Carbon and nitrogen isotope variations in tree-rings as records of perturbations in regional carbon and nitrogen cycles. *Environmental Science and Technology*, **41**, 1331–1338.

Cernusak LA, Tcherkez G, Keitel C, *et al.* (2009) Why are non-photosynthetic tissues generally ^{13}C enriched compared to leaves in C3 plants? Review and synthesis of current hypotheses. *Functional Plant Biology*., **36**, 199–213.

Choi WJ, Lee SM, Chang SX, Ro HM (2005) Variations of $\delta^{13}C$ and $\delta^{15}N$ in *Pinus densiflora* tree-rings and their relationship to environmental changes in eastern Korea. *Water Air and Soil Pollution*, **164**, 173–187.

Dail DB, Hollinger DY, Davidson EA, Fernandez I, Sievering HC, Scott NA, Gaige E (2009) Distribution of nitrogen 15-tracers applied to the canopy of a mature spruce-hemlock stand, Howland, Maine, USA. *Oecologia*, **160**, 589–599.

De Blij HJ, Muller PO, Williams RS, Williams RS Jr . (2004) *Physical Geography of the Global Environment*, **Volume 1**. Oxford University Press, Oxford.

Dentener F, Drevet J, Lamarque JF, *et al.* (2006) Nitrogen and sulfur deposition on regional and global scales: a multimodel evaluation. *Global Biogeochemical Cycles*, **20**, 1–21.

Dezi S, Medlyn BE, Tonon G, Magnani F (2010) The effect of nitrogen deposition on forest carbon sequestration: a model-based analysis. *Global Change Biology*, **16**, 1470–1486.

Diefendorf AF, Mueller KE, Wing SL, Koch PL, Freeman KH (2010) Global patterns in leaf ^{13}C discrimination and implications for studies of past and future climate. *Proceedings of the National Academy of Sciences USA*, **107**, 5738–5743.

Dongarrà G, Varrica D (2002) $\delta^{13}C$ variations in tree rings as an indication of severe changes in the urban air quality. *Atmospheric Environment*, **36**, 5887–5896.

Duquesnay A, Bréda N, Stievenard M, Dupouey JL (1998) Changes of tree-ring $\delta^{13}C$ and water-use efficiency of beech (*Fagus sylvatica* L.) in north-eastern France during the past century. *Plant, Cell and Environment*, **21**, 565–572.

Ehleringer JR, Cerling TE (1995) Atmospheric CO_2 and the ratio of intercellular to ambient CO_2 concentrations in plants. *Tree Physiology*, **15**, 105–111.

Epstein S, Krishnamurthy RV (1990) Environmental information in the isotopic record in trees. *Phylosphical Transaction of the Royal Society London A*, **330**, 427–439.

Farquhar GD, Ehlinger JR, Hubrick KT (1989) Carbon isotope discrimination and photosynthesis. *Annual Review of Plant Physiology and Plant Molecular Biology*, **40**, 503–537.

February EC, Stock WD (1999) Declining Trend in the $^{13}C/^{12}C$ Ratio of Atmospheric Carbon Dioxide from Tree Rings of South African *Widdringtonia cedarbergensis*. *Quaternary Research*, **52**, 229–236.

Feng X (1999) Trends in intrinsic water-use efficiency of natural trees for the past 100–200 years: a response to atmospheric CO_2 concentration. *Geochimica Cosmochimica Acta*, **63**, 1891–1903.

Feng X, Epstein S (1995) Carbon isotopes of trees from arid environments and implications for reconstructing atmosphere CO_2 concentration. *Geochimica Cosmochimica Acta*, **59**, 2599–2608.

Freckleton RP (2010) Dealing with collinearity in behavioural and ecological data: model averaging and the problems of measurement error. *Behavioral Ecology and Sociobiology*, **65**, 91–101.

Gaige E, Dail DB, Hollinger DY *et al.* (2007) Changes in canopy processes following whole-forest canopy nitrogen fertilization of a mature spruce-hemlock forest. *Ecosystems*, **10**, 1133–1147.

Galloway JN, Townsend AR, Erisman JW, *et al.* (2008) Transformation of the nitrogen cycle: recent trends, questions, and potential solutions. *Science*, **320**, 889–892.

Giuggiola A, Kuster TM, Saha S (2010) Drought-induced mortality of Scots pines at the southern limits of its distribution in Europe: causes and consequences. *iForest - Biogeosciences and Forestry*, **3**, 95–97.

Graham MH (2003) Confronting Multicollinearity in Ecological Multiple Regression. *Ecology*, **84**, 2809–2815.

Gruber N, Galloway J (2008) An Earth-system perspective of the global nitrose cycle. *Nature*, **451**, 293–296.

Guehl JM, Fort C, Ferhi A (1995) Differential response of leaf conductance, carbon isotope discrimination and water-use efficiency to nitrogen deficiency in maritime pine and pedunculate oak plants. *New Phytologist*, **13**, 149–157.

Guerrieri R, Mencuccini M, Sheppard LJ *et al.* (2011) The legacy of enhanced N and S deposition as revealed by the combined analysis of $\delta^{13}C$, $\delta^{18}O$ and $\delta^{15}N$ in tree rings. *Global Change Biology*, **17**, 1946–1962.

Guo R, Lin Z, Mo X (2010) Responses of crop yield and water use efficiency to climate change in the North China Plain. *Agricultural Water Management*, **97**, 1184–1193.

Harrison A, Schulze E-D, Gebauer G, Bruckner G (2000) Canopy uptake and utilization of atmospheric pollutant nitrogen. In *Carbon and Nitrogen Cycling in European Forest Ecosystems* (ed. Schulze E-D), pp. 171–188. Springer Verlag, Berlin.

Hastie TJ, Tibshirani RJ (1990) *Generalized Additive Models*. Chaman & Hall, New York.

Hemming DL, Switsur VR, Waterhouse JS, Heaton THE, Carter AHC (1998) Climate variation and the stable carbon isotope composition of tree ring cellulose: an intercomparison of *Quercus robur*, *Fagus sylvatica* and *Pinus silvestris*. *Tellus*, **50B**, 25–33.

Hietz P, Wanek W, Dünisch O (2005) Long-term trends in cellulose $\delta^{13}C$ and water-use efficiency of tropical *Cedrela* and *Swietenia* from Brazil. *Tree Physiology*, **25**, 745–752.

Högberg P, Johannisson C, Hällgren J-E (1993) Studies of ^{13}C in the foliage reveal interactions between nutrients and water in forest fertilization experiments. *Plant and Soil*, **152**, 207–214.

IAEA (1995) TECDOC- 825. Reference and intercomparison materials for stable isotopes of light elements, *Proceedings of a Consultants Meeting*, December 1–3, 1993, Vienna.

IPPC (2007) *Fourth Assessment Report. Chapter 10. Global climate projections. 10.7 Long Term Climate Change and Commitment 10.7.1, Climate Change Commitment to Year 2300. Based on AOGCM*, pp. 822, Cambridge University Press, Cambridge, United Kingdom and New York, NY, USA.

Jackson RB, Jobbagy EG, Avissar R *et al.* (2005) Trading water for carbon with biological carbon sequestration. *Science*, **310**, 1944–1947.

Jedrysek MO, Marek Krapiec M, Grzegorz Skrzypek G, Kałuzny A (2002) Air-pollution effect and paleotemperature scale versus δ13C records in tree rings and in a peat core (Southern Poland). *Water, Air, and Soil Pollution*, **145**, 359–375.

Kirdyanov AV, Treydte KS, Nikolaev A, Helle G, Schleser GH (2008) Climate signals in tree-ring width, density and δ13C from larches in Eastern Siberia (Russia). *Chemical Geology*, **252**, 31–41.

Kitagawa H, Matsumtoto E (1993) $\delta^{13}C$ records of Japanese cedars from Yakushima Island and past atmospheric CO_2. *Geochemical Journal*, **27**, 397–402.

Kohn MJ (2010) Carbon isotope compositions of terrestrial C_3 plants as indicators of (paleo)ecology and (paleo)climate. *Proceedings of the National Academy of Sciences USA*, **107**, 19691–19695.

Körner C (2006) Plant CO_2 responses: an issue of definition, time and resource supply. *New Phytologist*, **172**, 393–411.

Kremenetski KV, Boettgerc T, MacDonalda GM, Vaschalovad T, Sulerzhitskye L, Hillerf A (2004) Medieval climate warming and aridity as indicated by multiproxy evidence from the Kola Peninsula, Russia. *Palaeogeography, Palaeoclimatology, Palaeoecology*, **209**, 113–125.

Lamarque J-F, Bond TC, Eyring V, *et al.* (2010) Historical (1850–2000) gridded anthropogenic and biomass burning emissions of reactive gases and aerosols: methodology and application. *Atmospheric Chemistry and Physics*, **10**, 7017–7039.

Leavitt SW, Lara A (1994) South America tree show declining $\delta^{13}C$ trend. *Tellus*, **46B**, 152–157.

Leavitt SW, Long A (1988) Stable carbon isotope chronologies from trees in the southwestern United States. *Global Biogeochemical Cycles*, **2**, 189–198.

Leavitt SW, Long A (1989) The atmospheric $\delta^{13}C$ record as derived from 56 Pinyon trees at 14 sites in the Southwestern United States. *Radiocarbon*, **31**, 469–474.

Leavitt SW, Long A (1992) Altitudinal difference in δ13C of bristlecone pine tree rings. *Naturwissenschaften*, **79**, 178–180.

Loader NJ, Robertson I, McCarroll D (2003) Comparison of stable carbon isotope ratios in the whole wood, cellulose and lignin of oak tree-rings. *Palaeogeography, Palaeoclimatology, Palaeoecology*, **196**, 395–407.

Loader NJ, McCarroll D, Gagen M, Robertson I, Jalkanen R (2007) Extracting Climatic Information from Stable Isotope in Tree Rings. In: *Stable Isotopes as Indicators of Ecological Change*(eds Dawson TE, Siegwolf RTW), pp. 27–48, Terrestrial Ecology Series, Elsevier Inc., Amsterdam, Boston.

Magnani F, Mencuccini M, Borghetti M *et al.* (2007) The human footprint in the carbon cycle of temperate and boreal forests. *Nature*, **447**, 848–850.

Masson-Delmotte V, Raffalli-Delerce G, Danis PA, *et al.* (2005) Changes in European precipitation seasonality and in drought frequencies revealed by a four-century-long tree-ring isotopic record from Brittany, western France. *Climate Dynamics*, **24**, 57–69.

McCarroll D, Loader NJ (2004) Stable isotope in tree rings. *Quaternary Science Reviews*, **23**, 771–801.

McCarroll D, Gagen MH, Loader NJ *et al.* (2009) Correction of tree ring stable carbon isotope chronologies for changes in the carbon dioxide content of the atmosphere. *Geochimica et Cosmochimica Acta*, **73**, 1539–1547.

Monserud RA, Marshall JD (2001) Time-series analysis of $\delta^{13}C$ from tree rings: i Time trends and autocorrelation.. *Tree Physiology*, **21**, 1087–102.

Nakatsuka A, Ohnishi K, Hara T, Sumida A, Mitsuishi D, Kurita N, Uemura S (2004) Oxygen and carbon isotopic ratios of tree-ring cellulose in a conifer-hardwood mixed forest in northern Japan. *Geochemical Journal*, **38**, 77–88.

Neirynck J, Kowalski AS, Carrara A, Genouw G, Berghmans P, Ceulemans R (2007) Fluxes of oxidised and reduced nitrogen above a mixed coniferous forest exposed to various nitrogen emission sources. *Environmental Pollution*, **149**, 31–43.

Norby RJ (1998) Nitrogen deposition: a component of global change analyses. *New Phytologist*, **139**, 189–200.

Oliver RJ, Finch JW, Taylor G (2009) Second generation bioenergy crops and climate change: a review of the effects of elevated atmospheric CO_2 and drought on water use and the implications for yield. *GCB Bioenergy*, **1**, 97–114.

Ollinger SV, Aber JD, Reich PB, Freuder RJ (2002) Interactive effects of nitrogen deposition, tropospheric ozone, elevated CO_2 and land use history on the carbon dynamics of northern hardwood forests. *Global Change Biology*, **8**, 545–562.

Peñuelas J, Azcón-Bieto J (1992) Changes in leaf $\Delta^{13}C$ of herbarium plant species during the last 3 centuries of CO_2 increase. *Plant, Cell and Environment*, **15**, 485–489.

Peñuelas J, Hunt JM, Ogaya R, Jump AS (2008) Twentieth century changes of tree-ring $\delta^{13}C$ at the southern range-edge of *Fagus sylvatica*: increasing water-use efficiency does not avoid the growth decline induced by warming at low altitudes. *Global Change Biology*, **14**, 1076–1088.

Peñuelas J, Canadell JG, OgayaR (2011) Increased water-use efficiency during the 20th century did not translate into enhanced tree growth. *Global Ecology and Biogeography*, **20**, 597–608.

Pinheiro JC, Bates DM (2000) *Mixed-effects models in S and S-PLUS*. Springer Verlag, Berlin.

Pregitzer KS, Burton AJ, Zak DR, Talhelm AF (2008) Simulated chronic nitrogen deposition increases carbon storage in Northern Temperate forests. *Global Change Biology*, **14**, 142–153.

R Development Core Team (2011) *R A Language and Environment for Statistical Computing*. R Foundation for Statistical Computing, Vienna Austria, URL: http://www.R-project.org.

Raffalli-Delerce G, Masson-Delmotte V, Dupouey JL, Stievenard M, Breda N, Moisselin JM (2004) Reconstruction of summer droughts using tree-ring cellulose isotopes: a calibration study with living oaks from Brittany (western France). *Tellus*, **56B**, 160–174.

Reynolds-Henne CE, Siegwolf RTW, Treydte KS, Esper J, Henne S, Saurer M (2007) Temporal stability of climate-isotope relationships in tree rings of oak and pine (Ticino, Switzerland). *Global Biogeochemical Cycles*, **21**, 1–12.

Ripullone F, Lauteri M, Grassi G, Amato M, Borghetti M (2004) Variation in nitrogen supply changes the water use efficiency of *Pseudotsuga menziesii* and *Populus* x *euroamericana*; a comparison of three different approaches to determine water-use efficiency. *Tree Physiology*, **24**, 671–679.

Sakata M, Kiyoshi S (2000) Evaluating possible causes for the decline of Lapanese fir (Abies firma) forests based on $\delta^{13}C$ records of annual growth rings. *Environmental Science and Technology*, **34**, 373–376.

Sakata M, Kiyoshi S, Tadashi K (2001) Variations of wood $\delta^{13}C$ for the past 50 years in declining Siebold's beech (*Fagus crenata*) forests. *Environmental and Experimental Botany*, **45**, 33–41.

Saurer M, Siegwolf RTW (2007) Human impacts on tree-ring growth reconstructed from stable isotopes. In: *Stable Isotopes as Indicators of Ecological Change* (eds Dawson TE, Siegwolf RTW), pp. 49–62, Terrestrial Ecology Series, Elsevier Inc., Amsterdam, Boston.

Saurer M, Borella S, Schweingruber F, Siegwolf R (1997) Stable carbon isotopes in tree rings of beech: climatic versus site-related influences. *Trees*, **11**, 291–297.

Saurer M, Siegwolf RTW, Schweingruber FH (2004) Carbon isotope discrimination indicates improving water-use efficiency of trees in northern Eurasia over the last 100 years. *Global Change Biology*, **10**, 2109–2120.

Schielzeth H (2010) Simple means to improve the interpretability of regression coefficients. *Methods in Ecology and Evolution*, **2**, 103–113.

Schimel DS, House JI, Hibbard KA, *et al.* (2001) Recent patterns and mechanisms of carbon exchange by terrestrial ecosystems. *Nature*, **414**, 169–172.

Schlesinger WH (2009) On the fate of anthropogenic nitrogen. *Proceedings of the National Academy of Sciences USA*, **106**, 203–208.

Schultz MG, Backman L, Balkanski Y, *et al.* (2007) *REanalysis of the TROpospheric chemical composition over the past 40 years (RETRO) - A long-term global modeling study of tropospheric chemistry*. Final Report. Jülich GmbH, Hamburg, ISSN 1614-1199, Germany.

Seibt U, Rajabi A, Griffiths H, Berry JA (2008) Carbon isotopes and water use efficiency: sense and sensitivity. *Oecologia*, **155**, 441–454.

Serengil Y, Augustaitis A, Bytnerowicz A, *et al.* (2011) Adaptation of forest ecosystems to air pollution and climate change: a global assessment on research priorities. *iForest-Biogeosciences and Forestry*, **4**, 44–48.

Sheppard LJ, Crossley A, Harvey FJ, Skiba U, Coward P, Ingleby K (2004) Effects of five years of frequent N additions, with or without acidity, on the growth and below-ground dynamics of a young Sitka spruce stand growing on an acid peat: implications for sustainability. *Hydrology and Earth System Sciences*, **8**, 377–391.

Sheppard LJ, Crossley A, Ingleby K, Woods C (2008) Implications of acidified S inputs on the fate and consequences of N deposition: results from a field manipulation of a Sitka spruce canopy in southern Scotland. *International Journal of Environmental Studies*., **65**, 411–432.

Sievering H, Tomaszewski T, Torizzo J (2007) Canopy uptake of atmospheric N deposition at a conifer forest. Part I - Canopy N budget, photosynthetic efficiency and net ecosystem exchange. *Tellus B*, **59**, 483–492.

Sparks JD (2009) Ecological ramifications of the direct foliar uptake of nitrogen. *Oecologia*, **159**, 1–13.

Stuiver M, Burk RL, Quay PD (1984) $^{13}C/^{12}C$ ratios in tree rings and the transfer of biospheric carbon to the atmosphere. *Journal of Geophysical Research*, **89**, 11731–11748.

Sutton MA, Simpson D, Levy PE, Smith RI, Reis S, van Oijen M, De Vries W (2008) Uncertainties in the relationship between atmospheric nitrogen deposition and forest carbon sequestration. *Global Change Biology*, **14**, 1–7.

Szczepanek M, Pazdur A, Pawelczyk S *et al.* (2006) Hydrogen, Carbon And Oxygen Isotopes in Pine and oak tree rings from southern Poland as climatic indicators in years 1900–2003. *Geochronometria*, **25**, 67–76.

Thomas RQ, Canham CD, Weathers KC, Goodale CL (2010) Increased tree carbon storage in response to nitrogen deposition in the US. *Nature Geoscience*, **3**, 13–17.

Tognetti R, Johnson JD (1999) The effect of elevated atmospheric CO_2 concentration and nutrient supply on gas exchange, carbohydrates and foliar phenolic concentration in live oak (*Quercus virginiana* Mill.) seedlings. *Annals of Forest Science*, **56**, 379–389.

Treydte K, Schleser GH, Schweingruber FH (2001) The climatic significance of δ13C in subalpine spruces (Lotschental, Swiss Apls). *Tellus*, **53B**, 593–611.

Voronin VI, Schleser GH, Helle G (2001) Tree-ring stable carbon isotopes of Siberian larch as indicators of changing atmospheric CO_2 and humidity. In: *Proceedings of the International Conference Tree Rings and People* (eds Dobbertin KM, Bra ker OU), pp. 1–2, Swiss Federal Research Institute WSL, Birmensdorf, CH.

Waterhouse JS, Switsur VR, Barker AC, Carter AHC, Hemming DL, Loader NJ, Robertson J (2004) Northern European trees show a progressively diminishing response to increasing atmospheric carbon dioxide concentrations. *Quaternary Science Reviews*, **23**, 803–810.

Wittig VE, Ainsworth EA, Long SP (2007) To what extent do current and projected increases in surface ozone affect photosynthesis and stomatal conductance of trees? A meta-analytic review of the last 3 decades of experiments. *Plant Cell and Environment*, **30**, 1150–62.

Wittig VE, Ainsworth EA, Naiduz SL, Kanoski DF, Long SP (2009) Quantifying the impact of current and future tropospheric ozone on tree biomass, growth, physiology and biochemistry: a quantitative meta-analysis. *Global Change Biology*, **15**, 396–424.

Zhang Y, Chen T, An L, Li Y (2007) The variations of stable-carbon isotope ratios in Qilian juniper in northwestern China. *Environmental Geology*, **52**, 131–136.

Supporting Information

Additional Supporting Information may be found in the online version of this article:

Table S1. Mean latitude of sites and age of trees (average of trees' ages sampled in different sites, as reported in the original articles) trough the period 1950–2003.
S1supporting text. Materials and Methods. Assessing the effects of *iWUE* uncertainty on model results.
Figure S1. Variation in mean annual temperature (a), total annual precipitation (b) and numbers of wet days in a year (c) over the period 1950–2000 at the considered sites.
Figure S2. Correlation scatter plot of climatic and atmospheric variables in the data set; C_a: atmospheric carbon dioxide concentration; T_m: mean annual temperature; P: annual precipitation; D_w: number of wet days; N_{rate}: annual rate of N deposition; N_{cum}: cumulative N deposition; SO_x: annual rate of sulfur deposition; O_3: annual rate of tropospheric ozone deposition.
Figure S3. Variation in carbon isotope ratio ($\delta^{13}C$) between 1850 and 2000. Each point represents the mean of all tree chronologies for a given year. In the upper panel (a) empty circles represent angiosperms, in the lower panel (b) filled circles represent conifers. Vertical bars are ± 1.96 standard error. The continuous line corresponds to a locally weighed polynomial regression.
Figure S4. Variation in carbon isotope discrimination ($\Delta^{13}C$) as a function of rising level of CO_2 over the industrial period (1850–2000) for angiosperm (a) and conifer (b) species. Lines represent the theoretical changes of $\Delta^{13}C$ to increased atmospheric concentrations of CO_2 (C_a) according to the scenarios by Saurer *et al.* (2004): a totally passive response (scenario 1, dashed line), a constant ratio between intercellular (C_i) and atmospheric CO_2 concentration (scenario 2, horizontal straight line), a constant C_i (scenario 3, dotted line). The continuous line corresponds to a locally weighed polynomial regression. Each point represents the mean of all tree chronologies of the corresponding species for a given year; vertical bars are ± 1.96 SE.
Figure S5. Generalized Additive Modeling (GAM) results of mean annual temperature effects, panels (a) and (b), and total annual precipitation effects, panels (c) and (d), on intrinsic water-use efficiency (*iWUE*). The *y*-axis values indicate the *x*-axis covariate effect on the *iWUE* deviation from the mean predicted by the model (continuous line). Symbols are partial residuals around predicted covariate effects; empty circles for angiosperms, panels (a) and (c); filled circles for conifers, panels (b) and (d). The shaded areas indicate the 95% confidence interval. The number on each *y*-axis caption is the effective degrees of freedom for the term being plotted.
Figure S6. Tropospheric ozone concentration (a)) and SO_x deposition (b)) in the period 1950–2000. Circles represent the average values for the considered sites ($N = 53$); vertical bars are ± 1.96 SE.
Figure S7. Generalized Additive Modeling (GAM) results of SO_x deposition effects, panels (a) and (b), and O_3 deposition effects, panels (c) and (d), on intrinsic water-use efficiency (*iWUE*). Other covariates were mean annual temperature T_m, annual precipitation P, and atmospheric CO_2 concentration C_a. The *y*-axis values indicate the *x*-axis covariate effect on the *iWUE* deviation from the mean predicted by the model (continuous line). Symbols are partial residuals around predicted covariate effects; empty circles for angiosperms, panels (a) and (c); filled circles for conifers, panels (b) and (d). The shaded areas indicate the 95% confidence interval. The number on each *y*-axis caption is the effective degrees of freedom for the term being plotted.